Supporting Information

Mitchell *et al.* 10.1073/pnas.0804549105

SI Text

Clinical Samples. All clinical samples described here were obtained from subjects who had given informed consent, and studies were performed under the aegis of Institutional Review Board (IRB)-approved protocols.

Human donor blood samples used to generate data in Figs. 1 and 2, Fig. S1, and Fig. S3. Blood was collected from healthy donors in EDTA tubes (BD Biosciences 366643). All individuals were in good health based on self-report. Blood was processed for plasma isolation within 2 h of collection using the protocol described. Self-reported information on gender and prior history of cancer is given in Table S6.

Matched serum and plasma samples from healthy individuals used for analysis reported in Fig. 2C. Blood was collected from healthy women at increased risk of developing ovarian cancer (based on family history) who were participating in a Fred Hutchinson Cancer Research Center screening study for ovarian cancer early detection. Individuals did not have cancer at the time of sample collection or up to 2 years later. Plasma and serum samples were collected from each individual at the same draw. Ages of the women ranged from 45 to 55 years and all samples were collected in 2005. Blood was collected from consented study participants by a trained phlebotomist and processed within 4 hours of collection.

Serum samples from patients with prostate cancer and matched healthy controls reported in Fig. 4. Cancer samples were from patients with advanced (metastatic) prostate cancer and were obtained from patients being cared for at the University of Washington. Healthy controls were obtained from individuals undergoing prostate cancer screening including a digital rectal examination (DRE) and serum levels of PSA. Those subjects without suspicion of abnormalities (DRE) and within the normal range for serum PSA levels were consented as part of the normal healthy control subset. As far as possible, samples chosen were matched between cancer and control groups with respect to age of participants and duration of storage. All subjects were advised of the intent of the research study and those who agreed to participate signed a University of Washington Human Subject's Committee approved Informed Consent Form for a peripheral blood draw. Additional data pertaining to the serum samples obtained from prostate cancer patients and cancer-free controls are provided in Table S3.

Cell Culture. 22Rv1 human prostate cancer-derived cells were cultured in standard plastic tissue culture plates in RPMI medium 1640 (GIBCO) supplemented with 10% FBS and 1% penicillin-streptomycin at 37°C in a 5% CO_2 incubator. Primary prostate epithelial and primary prostate stromal cells were cultured as described (1).

Plasma Small RNA Library Construction and Sequencing. ***RNA isolation.*** Total RNA was prepared from human plasma from individual 006 (see Table S6) using a scaled-up version of the *mir*Vana PARIS (Ambion) protocol: 10 ml of plasma was thawed on ice, two 5-ml aliquots were transferred to 50-ml tubes, diluted with an equal volume of *mir*Vana PARIS 2X Denaturing Solution, mixed thoroughly by vortexing for 30 s and incubated on ice for 5 min. An equal volume (10 ml) of acid/phenol/chloroform (Ambion) was then added to each aliquot. The resulting solutions were vortexed for 1 min and spun for 5 min at 8,000 rpm, 20°C in a JA17 rotor. The acid/phenol/chloroform extraction was repeated three times. The resulting aqueous volume was mixed thoroughly with 1.25 volumes of 100% molecular-grade ethanol and passed through a *mir*Vana PARIS column in sequential 700-μl aliquots. The column was washed following the manufacturer's protocol, and RNA was eluted in 105 μl of elution buffer (95°C). A total of 1.5 μl of the eluate was quantified by Nanodrop. Approximately 250 ng of total plasma RNA was spiked with ~10 fmol (10,000 cpm) ^{32}P-labeled 18- and 24-nt RNA markers (Dharmacon) (2) and gel purified by electrophoresis through a 13-cm 15% denaturing polyacrylamide gel (National Diagnostics) at 300 V for 2 h 15 m (1×TBE). The 18- to 24-nt fraction was identified by phosphorimaging and excised with a scalpel. The subsequent gel slice was manually diced into smaller pieces and eluted in a 1.5-ml Eppendorf tube with shaking overnight at room temperature in 500 μl of 0.4 M NaCl. The eluate was filtered through a Pall Nanosep 0.2-μm spin filter for 5 min at 14,000 × *g*, room temperature. Twenty micrograms of glycogen and 1 ml of 100% molecular-grade ethanol were added to the filtrate and mixed by inversion, and RNA was precipitated overnight at −80°C. The precipitate was spun at maximum speed for 15 min, 4°C. The supernatant was removed by pipetting and the tube was spun again for 1 min. The remaining supernatant was removed, the precipitate was air-dried 2–3 min or until the pellet turned from white to clear and resuspended in 11 μl of RNase-free water.

3′ and 5′ ligations. Resuspended miRNA fractions were incubated in a 20 μl of reaction containing 5 μl of 50% PEG8000 (to 12.5%), 1 μl of 100 μM miRNA cloning linker 1 (IDT), and 1 μl (200 units) of NEB T4 Rnl2 (plus enzyme buffer) for 2 h at room temperature. Reactions were stopped with 20 μl of Gel Loading Buffer II (Ambion) and denatured for 5 min at 80°C before gel purification as above except through a 12% PAGE gel. The 35- to 41-nt 3′-ligated fraction was identified by phosphorimaging, excised, eluted, filtered, precipitated as above, and resuspended in 13 μl of water. 3′-ligated substrates were incubated in a 20-μl reaction with 2 μl of DMSO, 1 μl of 100 μM Illumina small-RNA cloning 5′linker (rGrUrUrCrArGrArGrUrUrCrUrArCrArGrUrCrCrGrArCrGrArUrC) and 2 μl of (20 units) Ambion T4 RNA ligase (plus enzyme buffer) for 1 h at 37°C. 5′-ligated substrates were denatured and gel purified as above except through a 10% PAGE gel. The 58- to 65-nt 5′-, 3′-ligated miRNA fraction was excised, eluted, filtered, precipitated as above, and resuspended in 20 μl of RNase-free water.

RT-PCR. Half (10 μl) of the 5′-, 3′-ligated miRNA solution was reverse-transcribed in a 20-μl reaction containing 1 M dNTPs, 10 μM DTT, 2 μl of 10 μM RT primer (CAAGCAGAAGACGGCATACGATTGATGGTGCCTACAG) and 1 μl of SuperScript RT III (Invitrogen) for 1 h at 50°C. Five microliters of cDNA was amplified in a 100-μl PCR using 1 μl each of 100 μM RT primer and forward primer (AATGATACGGCGACCACCGACAGGTTCAGAGTTCTACAGTCCGA) and Platinum Taq Polymerase High Fidelity (Invitrogen) for 15 cycles. PCR products of 105–110 bp were gel-purified through 4% metaphor agarose for 3.5 h at 120V and excised using a clean scalpel. PCR products were recovered by dissolving the agarose in 50 μl (total volume) of 0.4 M NaCl for 10 min at 70°C. Five hundred microliters of equilibrated phenol (pH 8.0) was added, followed by vortexing for ~30 s and spinning for 5 min at maximum speed. The resulting aqueous phase was extracted twice with phenol/chloroform/isoamyl alcohol, extracted with chloroform once, and precipitated with 20 μg glycogen and 1 ml of 100% ethanol at −80°C overnight. Precipitates were spun at maximum speed for 15 min at 4°C. The supernatant was removed by pipetting and

precipitates were spun again briefly. The remaining supernatant was removed, and pellets were air-dried for ~5 min, resuspended in 20 μl RNase-free water, and quantified by Nanodrop. One microliter of the PCR product was TOPO cloned (Invitrogen) and transformed into chemically competent *E. coli*. Transformants were screened by whole-cell PCR (50-μl reactions) using primers specific to pCR4-TOPO ~200 nt flanking the insertion site. Whole-cell PCR products were purified using a Qiagen 96-well PCR purification kit and sequenced by standard Sanger sequencing using a M13 forward primer.

Small RNA Library Generation from Prostate Epithelial and Stromal Cell Cultures and 454 Sequencing. Total RNA derived from two primary prostate epithelial cultures (149.1 μg in 120 μl) and from two primary stromal cell cultures (124.15 μg in 120 μl) was spiked with ^{32}P-labeled 18- and 24-nt markers and the 18- to 24-nt miRNA fraction was gel-purified, phosphorimaged, excised, eluted, filtered, precipitated, and resuspended in 13 μl of RNase-free water as described above. This fraction was then 3′-ligated for 2 h at room temperature in a 20 μl final volume with: 1 μl of Ambion T4 RNA ligase (10U); 4 μl 5X ligase buffer (250 mM Hepes, pH8.3; 50 mM $MgCl_2$; 16.5 mM DTT; 50 μg/ml BSA; 41.5% glycerol); 2 μl 100 μM miRNA cloning linker 1 (IDT). The 3′-ligated miRNA fraction was gel purified as above through 12% PAGE at 300V for 2.5 h. The 35- to 41-nt band was isolated and recovered as above, resuspended in 12 μl RNase-free water and 5′-ligated for 1 h at 37°C in a 20-μl final volume with: 2 μl Ambion T4 RNA ligase (20U); 2 μl 200 μM of the 5′linker (also known as 17.93R) (ATCGTrArGrGrCrArCrCrUrGrArArA); 2 μl 10X Ambion T4 RNA ligase buffer; 2 μl DMSO. 5′-, 3′-ligated substrates were gel purified as above through 10% PAGE at 300V for 2.5 h. The 52- to 58-nt fraction was recovered and resuspended in 12 μl. Four microliters of each of the fully ligated RNA samples was reverse-transcribed in a 29-μl reaction containing Invitrogen SuperScript RT III and buffer, 3.1 μM of RT primer (also known as primer 15.22) (ATTGATGGTGCCTAC) and 0.44 mM dNTPs at 50°C for 1 h, followed by treatment with RNase H (Invitrogen) for 30 min at 37°C. One microliter of the reverse transcription product was PCR-amplified in a 100-μl reaction containing AmpliTaq Gold and buffer (Applied Biosystems), 1.9 mM $MgCl_2$, 250 μM dNTPs, and 1 μM each of primers 17.92 (5′PhosATTGATGGTGCCTACAG) and 17.93DG (5′PhosATCGTAGGCACCTGAGA) for 20 cycles (95°C for 30 s, 50°C for 30 s, 72°C for 90 s). PCR products were gel purified on 12% nondenaturing polyacrylamide gel. The gel was stained with Sybr Gold (Invitrogen) and bands of ≈50 bp were excised from the gel and eluted in 0.4 M sodium chloride by shaking overnight on a vortexer. Residual polyacrylamide gel pieces were removed by running the sample through a PALL Nanosep MF 0.2-μm filter. PCR products were precipitated overnight with 20 μg glycogen and 1,200 μl of ethanol. The precipitate was centrifuged for 30 min at 4°C at maximum speed and the supernatant was removed by pipetting. The pellet was air dried and resuspended in 20 μl of RNase-free water. One microliter of the first PCR products were then PCR amplified a second time in a 100-μl reaction containing AmpliTaq Gold and buffer, 1.5 mM $MgCl_2$, 200 μM dNTPS and 0.2 μM each of forward primer ''454A-5′L'' (5′GCCTCCCTCGCGCCATCAGATCGTAGGCACCTGAGA′3) and reverse primer "454B -3′L" (5′GCCTTGCCAGCCCGCTCAGATTGATGGTGCCTACAG′3). The PCR was carried out as follows: initial denaturation at 96°C for 60 s, then (96°C for 10 s, 50°C for 60 s, 72°C for 20 s) x 15 cycles, then 72°C extension for 3 min. Approximately 100-bp PCR products were gel purified after electrophoresis through a 3% metaphor agarose gel for 2 h at 110V and excision using a scalpel. PCR products were recovered with the QiaQuick Gel Extraction Kit (Qiagen) using the manufacturer's recommended protocol. Samples were eluted with 50 μl of elution buffer. Samples were quantified by both Nanodrop spectrophotometer and PicoGreen assay (Invitrogen) before sequencing by 454 Life Technolgies using a Genome Sequencer FLX.

The complete set of reads for the sequencing data obtained was compiled into a set of nonredundant sequences, with the number of reads for each sequence reflecting relative abundance. The PEC dataset contained 4,721 nonredundant sequences with 60,390 reads and the PSC dataset contained 4,307 nonredundant sequences with 32,829 reads. We compared our sequences against the set of known miRNAs in miRBase Release v.10. Reads for supersequences, subsequences or sequences having significant overlap with known miRNAs were incorporated into the total number of reads given in Table S4. We identified 131 known miRNAs in the PEC dataset and 122 known miRNAs in the PSC dataset.

Extraction and Representation of miRNA Profiling Data from the Lu *et al.* (3) Dataset. Given the $\log_2$ expression values for *miR-141* in all samples from the Lu *et al.* data (3), we first removed samples originating from cell lines, normal tissues or nonhuman sources. Data from the remaining samples, representing the human tumor tissues, were subjected to hierarchical clustering (average linkage, correlation similarity) to construct the heatmap shown in Fig. S6. Expression values ranged from 5 (black) to 11.8 (yellow).

Xenograft Experiments. All mouse experiments were performed in accordance with IACUC-approved protocols.

Mice. NOD/SCID mice (Strain NOD.CB17-*Prkdc*^{scid}/J, stock number 001303), were purchased from Jackson Labs and bred in-house (Core Center of Excellence in Hematology Core E. NOD/SCID Assay). The mice were housed at a density of five mice per cage in an SPF environment in laminate airflow units changed once per week. They were treated with 1 week on Septra 8 ml / 50 ml H_2O, 1 week off.

Injection of 22Rv1 human prostate cancer cells. Two cohorts of mice were established, staggered by 20 days. Each cohort was comprised of 12 xenografted mice and 12 control mice. 22Rv1 cells were harvested for injection with trypsin (0.05%)-EDTA solution, washed with culture medium and resuspended in a solution of ice-cold 50% basement membrane matrix (BD Matrigel) in HBSS (GIBCO) at a concentration of 7.5×10^6 cells/ml. Xenografts were established in 12 NOD/SCID mice by s.c. injection at the hip of 7.5×10^5 cells/mouse in 200 μl of total volume cell-Matrigel-HBSS suspension. An equal number of control mice (12 in all) received mock injections of 200 μl of 50% Matrigel in HBSS. Injections were carried out in batches of five mice, rotating between five xenografts, five controls, five xenografts, and so forth.

Blood and tumor tissue collection. In the first cohort, all 12 xenograft mice developed grossly visible tumors. Samples from this cohort were used to generate the data presented in Fig. 3. In the second cohort, all but one of the mice in the xenograft group developed a tumor. This cohort was used to generate the data presented in Fig. S5. No tumors developed in control mice in either cohort. All mice were killed 28 days postinjection. Before death, mice were anesthetized by an i.p. injection of 500 μl of Avertin and blood was collected in EDTA tubes (Sarstedt 41.1395.105) using cardiac puncture. This was followed by cervical dislocation. Each tumor was harvested in its entirety, snap frozen in liquid nitrogen, and stored at −80°C.

Mice were processed in groups of five (i.e., corresponding to one cage at a time), rotating between xenograft and control groups of mice. This alternating pattern was maintained throughout collection and processing of plasma and tissues to minimize potential bias caused by a batch effect related to the duration of time elapsed between collection of early and late

samples. Processing time from first cardiac puncture through last tumor harvest was 1 h, 45 min for the first cohort, 45 min for the second. Weights of the frozen tumors from the first cohort after harvest are provided in Table S7.

Blood Processing and Isolation of Serum and Plasma. ***Isolation of mouse plasma.*** Blood was processed within 1 h of collection by centrifugation at 1,300 × *g* at 4°C in a refrigerated microfuge for 10 min. Plasma was transferred to a fresh RNase/DNase-free 1.5-ml microfuge tube, leaving enough plasma in the original tube such that the lowest point of the meniscus did not touch the pellet. Plasma samples were stored at −80°C.

Isolation of human plasma for experiments shown in Figs. 1 and 2, and Fig. S1 and Fig. S3. Blood was collected from healthy donors in EDTA tubes (BD Biosciences 366643) and processed for isolation of plasma within 2 h of collection. At a given sitting, the amount of blood drawn ranged from ~20 to ~90 ml. Blood from several EDTA tubes was pooled and transferred to RNase/DNase-free 50-ml conical tubes (Greiner), and centrifuged at 1,200 × *g* at room temperature in a Hettich Rotanta 460R benchtop centrifuge for 10 min. Plasma was transferred to a fresh tube, leaving behind a fixed height of 0.5 cm plasma supernatant above the pellet to avoid disturbing the pellet. Plasma was aliquoted, with inversion to mix between each aliquot, and stored at −80°C. The exception for this was plasma miRNA stability studies reported in Fig. 2*A*, where freshly collected plasma was carried into the studies immediately rather than being frozen for storage initially.

Isolation of serum and plasma from matched samples used for analysis reported in Fig. 2C. Blood was collected from consented study participants by a trained phlebotomist. Up to 50 ml of whole blood was collected at the same draw for both serum (serum separator tube; SST) and plasma isolation (EDTA tube). For serum isolation, samples were allowed to sit at room temperature for at least 30 min between collection and centrifugation to allow the blood in the SST tubes to clot. Serum from the SST tubes was aliquoted into microcentrifuge tubes, 1 ml per aliquot. EDTA tubes were spun in a benchtop centrifuge at 1,200 × *g* for 10 min to separate the cells from the fluid. Plasma was aliquoted into microcentrifuge tubes, 1 ml per aliquot. Blood samples were processed and serum and plasma were frozen within 4 h of the blood draw. After aliquoting, plasma and serum were frozen on dry ice and subsequently stored at −80°C.

Serum samples from patients with prostate cancer and matched healthy controls. All peripheral blood samples were collected in a 10-ml Vacutainer SST Plus Blood Collection Tube (BD367985). Samples were allowed to sit at room temperature for a minimum of 30 min and a max of 2 h. Separation of the clot was accomplished by centrifugation at 1,000–1,300 × *g* at 4°C for 15–20 min. The serum was removed and dispensed in aliquots of 500 μl into 500- to 750-μl cryo-tubes. Specimens were stored at −80°C. Aliquots used for analysis of pools underwent two freeze-thaw cycles and those used for analysis of individual samples underwent three freeze-thaw cycles since the time of collection.

RNA Isolation Procedures. ***RNA isolation from cultured cells.*** Cells were washed twice with PBS. Six hundred microliters of Lysis/Binding buffer from the *mir*Vana miRNA isolation kit (Ambion 1560) was added directly to the culture plate or flask to lyse the cells. Lysates were harvested manually with a sterile cell scraper and transferred to a 2-ml tube. Samples were stored at −80°C or RNA was immediately extracted using the manufacturer's recommended protocol for total RNA isolation.

RNA isolation from mouse plasma samples. One hundred microliters of mouse plasma was thawed on ice and transferred to a tube containing 100 μl of H_2O and 200 μl of 2X Denaturing Solution (Ambion). To allow for normalization of sample-to-sample variation in the RNA isolation step, synthetic *C. elegans* miRNAs *cel-miR-39*, *cel-miR-54*, and *cel-miR-238* (synthetic RNA oligonucleotides synthesized by Qiagen) were added (as a mixture of 25 fmol of each oligonucleotide in a 5-μl total volume) to each denatured sample (i.e., after combining the plasma sample with Denaturing Solution). RNA was isolated using the *mir*Vana PARIS kit following the manufacturer's protocol for liquid samples (Ambion), modified such that samples were extracted twice with an equal volume of acid-phenol chloroform (as supplied by the Ambion kit). RNA was eluted with 105 μl of water. The average volume of eluate recovered from each column was 80 μl.

RNA isolation from human plasma and serum samples. For all experiments, 400 μl of human plasma or serum was thawed on ice and lysed with an equal volume of 2X Denaturing Solution (Ambion). In the case of serum pools used for screening human prostate cancer biomarker candidates (Table S2), pools were created by combining 20 μl of each of 25 samples. The pools were mixed by inversion and 400 μl was transferred to a new tube for RNA isolation. To allow for normalization of sample-to-sample variation in RNA isolation, synthetic *C. elegans* miRNAs *cel-miR-39*, *cel-miR-54*, and *cel-miR-238* (synthetic RNA oligonucleotides synthesized by Qiagen) were added (as a mixture of 25 fmol of each oligonucleotide in a 5-μl total volume) to each denatured sample (i.e., after combining the plasma sample with Denaturing Solution) with the exception of samples for experiments shown in Fig. 2*B* that were intended to test for endogenous plasma RNase activity. RNA was isolated using the *mir*Vana PARIS kit following the manufacturer's protocol for liquid samples (Ambion), modified such that samples were extracted twice with an equal volume of acid-phenol chloroform (as supplied by the Ambion kit). RNA was eluted with 105 μl of Ambion elution solution according to the manufacturer's protocol. The average volume of eluate recovered from each column was 80 μl.

Measurement of miRNA Levels in RNA from Plasma and Serum by Using *Taq*Man qRT-PCR Assays. ***Procedure for miRNA assay of RNA isolated from serum or plasma.*** A fixed volume of 1.67 μl of RNA solution from the ~80 μl-eluate from RNA isolation of a given sample was used as input into the reverse transcription (RT) reaction. For samples in which RNA was isolated from a 400-μl plasma or serum sample, for example, 1.67 μl of RNA solution represents the RNA corresponding to (1.67/80) × 400 = 8.3 μl plasma or serum. For generation of standard curves of chemically synthesized RNA oligonucleotides corresponding to known miRNAs, varying dilutions of each oligonucleotide were made in water such that the final input into the RT reaction had a volume of 1.67 μl.

Input RNA was reverse transcribed using the TaqMan miRNA Reverse Transcription Kit and miRNA-specific stem-loop primers (Applied BioSystems) in a small-scale RT reaction [comprised of 1.387 μl of H_2O, 0.5 μl of 10X Reverse-Transcription Buffer, 0.063 μl of RNase-Inhibitor (20 units /μl), 0.05 μl of 100 mM dNTPs with dTTP, 0.33 μl of Multiscribe Reverse-Transcriptase, and 1.67 μl of input RNA; components other than the input RNA were prepared as a larger volume master mix], using a Tetrad2 Peltier Thermal Cycler (BioRad) at 16°C for 30 min, 42°C for 30 min and 85°C for 5 min. For *miR-15b, miR-16*, *miR-19b*, and *miR-24* and *C. elegans* miRNAs, 2.25 μl of diluted RT product (prepared by combining 5.0 μl of RT product with 28.9 μl of H_2O) was combined with 2.75 μl of PCR assay reagents (comprised of 2.5 μl of TaqMan 2X Universal PCR Master Mix, No AmpErase UNG and 0.25 μl of TaqMan miRNA Assay) to generate a PCR of 5.0 μl of total volume. Real-time PCR was carried out on an Applied BioSystems 7900HT thermocycler at 95°C for 10 min, followed by 40 cycles of 95°C for 15 s and 60°C for 1 min. Data were analyzed with SDS Relative Quantification Software version 2.2.2 (Applied BioSystems.), with the auto-

matic Ct setting for assigning baseline and threshold for Ct determination.

For *miR-100*, *miR-125b*, *miR-141*, *miR-205*, *miR-296*, *miR-660*, and *miR-629**, the protocol was modified as follows to include a preamplification step. A 1.25-μl aliquot of undiluted RT product was combined with 3.75 μl of Preamplification PCR reagents [comprised, per reaction, of 2.5 μl of TaqMan PreAmp Master Mix (2X) and 1.25 μl of 0.2X TaqMan miRNA Assay (diluted in TE)] to generate a 5.0-μl preamplification PCR, which was carried out on a Tetrad2 Peltier Thermal Cycler (BioRad) by heating to 95°C for 10 min, followed by 14 cycles of 95°C for 15 s and 60°C for 4 min. The preamplification PCR product was diluted (by adding 20 μl of H_2O to the 5-μl preamplification reaction product), following which 2.25 μl of the diluted material was introduced into the real-time PCR and carried forward as described for the other miRNA assays above. Detailed information regarding miRNA Taqman assays used in this study is provided in Table S8.

Generation of standard curves for absolute quantification of miRNAs. Synthetic single-stranded RNA oligonucleotides corresponding to the mature miRNA sequence (miRBase Release v.10.1) were purchased from IDT (*miR-629**), Sigma (*miR-141* and *miR-660*) or Qiagen (*miR-15b*, *miR-16*, *miR-19b*, and *miR-24*). Sequence information is provided in Table S5. Synthetic miRNAs were input into the RT reaction over an empirically-derived range of copies to generate standard curves for each of the miRNA TaqMan assays listed above (representative standard curves for each assay are provided in Fig. S2). In general, the lower limit of accurate quantification for each assay was designated based on the minimal number of copies input into an RT reaction that resulted in a Ct value within the linear range of the standard curve and that was also not equivalent to or higher than a Ct obtained from an RT input of lower copy number. A line was fit to data from each dilution series using Ct values within the linear range, from which $y = \mathrm{mln}(x) + b$ equations were derived for quantification of absolute miRNA copies (x) from each sample Ct (y). Absolute copies of miRNA input into the RT reaction were converted to copies of miRNA per microliter plasma (or serum) based on the knowledge that the material input into the RT reaction corresponds to RNA from 2.1% of the total starting volume of plasma [i.e., 1.67 μl of the total RNA eluate volume (80 μl on average) was input into the RT reaction].

The layout of samples in the RT, preamplification, and real-time PCR reactions in strip tubes and multiwell plates was designed to minimize the chance of cross-contamination by standard curve samples and to minimize systematic bias when comparing groups such as xenografted mice and control mice. Whenever possible, experimental samples were separated from standard curves by at least one empty row. In the mouse xenograft experiments, RNA samples from xenografts and controls were blinded and randomized in layout on the PCR plate. In the human xenograft experiments, case and control samples were alternated in sequence to avoid bias related to geographic location on the PCR plate.

Normalization of Experimental qRT-PCR Data Using Spiked-In *C. elegans* miRNAs as Controls. Given the early stage of plasma/serum miRNA research, no established endogenous small RNA control exists for normalization of technical variations in sample processing or of potential variation in sample quality (i.e., presence of PCR inhibitors due to occult red blood cell lysis in plasma samples, for example). Normalizing by matching the amount of input RNA into the RT reaction is not an appropriate approach because the RNA content of plasma can vary considerably and in fact has been suggested to vary with disease states. We therefore chose to use a fixed volume of RNA eluate (1.67 μl) from a given volume of starting plasma, rather than a fixed mass of RNA, as input into the RT reaction. For example, for a sample in which the starting plasma volume was 400 μl, an input of 1.67 μl of eluted RNA (taken from a total RNA eluate volume of ~80 μl) into the RT reaction corresponds to the mass of RNA derived from ~8.3 μl of starting plasma.

We devised an approach for data normalization based upon spiking in three synthetic RNA oligonucleotides corresponding to miRNAs that do not exist in the mouse or human genomes. These RNAs were synthesized to match the sequence of three *C. elegans* miRNAs, *cel-miR-39*, *cel-miR-54*, and *cel-miR-238* (purchased as custom RNA oligonucleotide syntheses from Qiagen) and were confirmed empirically as not cross-hybridizing with probes for known human miRNAs on a locked nucleic acid-probe-based microRNA microarray (data not shown). The spiked-in oligos were introduced (as a mixture of 25 fmol of each oligonucleotide in a 5-μl total volume of water) after addition of 2X Denaturing Solution (Ambion) to the plasma or serum sample to avoid degradation by endogenous plasma RNases. For each RNA sample, the *C. elegans* spiked-in miRNAs were measured using TaqMan qRT-PCR assays (Applied Biosystems) as described earlier.

We normalized the data across samples using a median normalization procedure. For each sample, the Ct values obtained for the three spiked-in *C. elegans* miRNAs were averaged to generate SpikeIn_Average_Ct value. The median of the SpikeIn_Average_Ct values obtained from all of the samples to be compared was next calculated (designated here as the Median_SpikeIn_Ct value). A Normalization_Factor was then calculated for each sample based on the following formula: Normalization_Factor = 1/[2^(Median_SpikeIn_Ct value) − (SpikeIn_Average_Ct value of the given sample). The number of copies of a given miRNA in each sample (calculated using the standard curves described earlier) was multiplied by the Normalization_Factor corresponding to the sample to obtain a normalized copy number value. In cases where it was desirable to apply normalization directly to Raw_Ct values corresponding to miRNAs of interest (e.g., Fig. 2*A*), the Raw_Ct for a given miRNA in a given sample was adjusted as follows: Normalized_Ct value for the miRNA in the sample = Raw_Ct value − [(SpikeIn_Average_Ct value of the given sample) − (Median_SpikeIn_Ct value)].

miRNA Profiling Using *Taq*Man Low-Density Array miRNA qRT-PCR Technology. MiRNA expression in the 22Rv1 prostate cancer cell line and in a plasma sample of RNA from a healthy human donor (individual 006, Table S6) was profiled using TaqMan Human MicroRNA Arrays (v1.0), using the manufacturer's recommended protocol (Applied Biosystems.). This is a version of the TaqMan Low-Density Array (TLDA) qRT-PCR profiling platform. Briefly, the RNA was reverse transcribed using the TaqMan MiRNA Reverse Transcription Kit, and the TaqMan MiRNA Multiplex RT Assays, Human Pool Set. One-hundred nanograms of 22Rv1 RNA or 2 μl of human plasma RNA was added to each of the eight multiplex reverse transcription reactions. Multiplex RT reactions were diluted 62.5-fold with water, and 55 μl of each diluted product was combined with 55 μl of TaqMan 2X Universal PCR Master Mix, No AmpErase UNG. One-hundred microliters of the sample/master mix for each Multiplex pool was loaded into the array, the array was then centrifuged and mechanically sealed with the Applied Biosystems sealer device. qRT-PCR was carried out on an Applied BioSystems 7900HT thermocycler using the manufacturer's recommended cycling conditions. Data were analyzed with SDS Relative Quantification Software version 2.2.2 (Applied BioSystems), with an assigned minimum threshold of 0.123518, which was above the baseline of all assays showing measurable amplification above background.

Selection of Prostate Cancer miRNA Biomarker Candidates. To identify candidate serum miRNA biomarkers for prostate cancer, we began by examining human prostate cancer miRNA expression data from the large cancer miRNA profiling dataset of Lu *et al.* (3). In this dataset, 126 of the 151 miRNAs profiled were detectable across prostate cancer samples (with detectable expression defined as $\log_2$ expression value >5). We next intersected this list of 126 miRNAs with results from a prostate cancer miRNA profiling study published by Porkka *et al.* (4), which yielded 40 miRNAs that were detected in prostate cancer samples in both studies. Reasoning that an ideal miRNA cancer biomarker candidate should have low or absent expression in plasma from healthy individuals, we compiled a list of miRNAs detectable at baseline in normal human plasma by (*i*) examining the list of miRNAs identified in the plasma miRNA experiment reported in Fig. 1*A* (with methods as described), and (*ii*) miRNA profiling of healthy-donor plasma using a TaqMan Human MiRNA Array v1.0 (this is a moderate-sensitivity TaqMan qRT-PCR-based platform for miRNA profiling; data from this profiling experiment are provided in Table S9). We removed from our list of biomarker candidates any miRNAs that were sequenced in the plasma miRNA cloning study or that were detected at any Ct value in the plasma TaqMan miRNA qRT-PCR Array experiment. These procedures yielded a list of six miRNA biomarker candidates: *miR-100*, *miR-125b*, *miR-141*, *miR-143*, *miR-205*, and *miR-296*, which were measured in RNA samples derived from pools of prostate cancer cases and controls as described earlier.

Characterization of the Stability of miRNAs in Plasma by Prolonged Incubation at Room Temperature and Subjection to Repetitive Freeze–Thaw Cycles. Human plasma from individuals 006 and 008 (plasma donors described in Table S6) was isolated from whole blood as described. Four hundred-microliter aliquots of plasma freshly isolated from each individual were maintained at room temperature for 30 min, 1 h, 2 h, 4 h, 8 h, and 24 h in 2-ml RNase/DNase-free tubes. Experiments were carried out using duplicate plasma aliquots for each time point from each individual. Immediately after completion of an incubation period, samples were processed for RNA isolation by addition of an equal volume (400 μl) 2X Denaturing Solution (Ambion), vortexing for 5 min, placing on ice for 5 min (per the manufacturer's protocol) followed by spike in of normalization control miRNA oligos and further RNA isolation as described. Measurement of levels of endogenous human miRNAs and normalization control miRNAs was carried out by qRT-PCR as described and data normalization was performed as described.

To assess the stability of miRNAs in plasma to multiple freeze-thaw cycles, 10 400-μl aliquots of freshly isolated plasma from each of the two individuals described above (and from the same plasma batches) as described above were procured for experimentation. Two aliquots corresponding to each individual were initially removed (representing the 0X freeze-thaw samples) and processed for RNA isolation by addition of an equal volume (400 μl) 2X Denaturing Solution (Ambion), vortexing for 5 min, placing on ice for 5 minutes (per the manufacturer's protocol) followed by addition of spiked in normalization control miRNA oligos and further RNA isolation as described. The remaining aliquots were frozen by placing on dry ice for 10 min. Plasma aliquots were then allowed to thaw at room temperature for 20 min after which two duplicate aliquots corresponding to each individual were removed (1X freeze-thaw samples) and processed for RNA isolation and addition of spiked in normalization control miRNA oligos as detailed above. The remaining samples were frozen again by placing on dry ice for 10 min, following which the thawing procedure was repeated and two duplicate aliquots from each individual were removed (2X freeze-thaw samples) for RNA isolation and addition of spiked in normalization control miRNA oligos as detailed above. The freeze-thaw procedure described above was reiterated until 4X and 8X freeze-thaw samples had been collected and processed in a manner identical to that detailed above. Measurement of levels of endogenous human miRNAs and normalization control miRNAs was carried out by qRT-PCR as described and data normalization was performed as described.

Demonstration of Sensitivity of Synthetic, Exogenous miRNAs to Plasma RNase Activity (and Resistance of Endogenous miRNAs) Using Synthetic Oligo Spike-In Before or After Plasma Denaturation. Plasma from individual 003 (plasma donor described in Table S6) was isolated from whole blood as described. Two 400-μl aliquots were thawed and used for the experiment described here. Synthetic RNA oligonucleotides corresponding to *C. elegans* miRNAs *cel-miR-39*, *cel-miR-54*, and *cel-miR-238* (purchased as custom RNA oligonucleotide syntheses from Qiagen) were added (as a mixture of 25 fmol of each oligonucleotide in a 5-μl total volume of water) to one plasma aliquot, followed <2 min later by addition of 400 μl of 2X Denaturing Solution, vortexing, and incubation on ice for 5 min. The other plasma aliquot was processed by first adding 400 μl of 2X Denaturing Solution, vortexing and incubating on ice for 5 min, after which the mixture of three synthetic *C. elegans* miRNAs described above was added. Denatured samples were carried through the remainder of the plasma RNA isolation procedure as described, followed by TaqMan qRT-PCR for measurement of the spiked-in miRNAs as well as endogenous miRNAs (results presented in Fig. 2*B*).

Characterization of Tumor-Derived miRNAs in Mouse Plasma by Differential Centrifugation. Frozen plasma from 22Rv1 xenografted or control NOD/SCID mice from the second cohort was thawed at room temperature. Two plasma pools were generated (one corresponding to xenograft mice and one corresponding to control mice) by combining equal volume aliquots of plasma from each mouse within a group, yielding a pool of total volume ~600 μl. Forty microliters of pooled plasma corresponding to xenograft or control groups was centrifuged serially at 2,000 × *g*, 20°C for 30 min and 12,000 × *g* at 20°C for 45 min in a 5415 R microcentrifuge (Eppendorf). Obviously visible pellets were not obtained; therefore all but ~10 μl of supernatant was removed to a new tube at each step to avoid disrupting any translucent pellets that might be difficult to visualize. Resulting "pellets" and the 12,000 × *g* supernatant were each brought to a 400-μl final volume in PBS, following which they were immediately denatured by the addition of 400 μl of 2X Denaturing Solution (Ambion) and vortexed to mix. Synthetic *C. elegans* miRNAs *cel-miR-39*, *cel-miR-54*, and *cel-miR-238* (purchased as custom RNA oligonucleotide syntheses from Qiagen) were then added (as a mixture of 25 fmol of each oligonucleotide in a 5 μl of total volume) with vortexing briefly to mix. RNA was isolated as described.

Characterization of Tumor-Derived miRNAs in Mouse Plasma by Microfiltration. Forty microliters of plasma pools corresponding to xenograft and control groups (aliquots of the same pools as generated for differential centrifugation experiments above) were brought to 100-μl final volume in PBS. Millex-GV 0.22-μm, 4.0-mm-diameter filter units (Millipore) were prewashed with 500 μl of PBS using a 1.0-ml BD Luer-Lok disposable syringe (Becton Dickinson). Each plasma pool was passed through filter unit using a fresh syringe, followed by filtration of an additional 250-μl volume of PBS as a wash that was collected and combined with the plasma filtrate and collectively designated as the Filtrate sample. With a fresh syringe, the Retentate was collected by passing 200 μl of 2X Denaturing Solution (Ambion) through filter unit, which was then incubated 10 min at room temperature followed by a second passage of 200 μl of 2X Denaturing Solution through the filter unit. The PVDF filter membrane was

the manually dissected from HDPE filter apparatus using a sterile scalpel and added into the Retentate flow-through sample. The Retentate samples were vortexed for 10 min to completely solubilize RNA from the filter unit. Retentate samples were briefly spun and then brought to 800 μl of final volume with PBS, to which synthetic *C. elegans* miRNAs *cel-miR-39*, *cel-miR-54*, and *cel-miR-238* (purchased as custom RNA oligonucleotide syntheses from Qiagen) were added (as a mixture of 25 fmol of each oligonucleotide in a 5-μl total volume). Filtrate samples were brought to 400-μl final volume in PBS and immediately denatured by addition of 400 μl of 2X Denaturing Solution. Samples were vortexed after which synthetic *C. elegans* miRNAs *cel-miR-39*, *cel-miR-54*, and *cel-miR-238* (purchased as custom RNA oligonucleotide syntheses from Qiagen) were added (as a mixture of 25 fmol of each oligonucleotide in a 5-μl total volume). RNA was isolated as described.

1. Gmyrek GA, *et al.* (2001) Normal and malignant prostate epithelial cells differ in their response to hepatocyte growth factor/scatter factor. *Am J Pathol* 159:579–590.
2. Lau NC, *et al.* (2001) An abundant class of tiny RNAs with probable regulatory roles in *Caenorhabditis elegans. Science* 294:858–862.
3. Lu J, *et al.* (2005) MicroRNA expression profiles classify human cancers. *Nature* 435:834–838.
4. Porkka KP, *et al.* (2007) MicroRNA expression profiling in prostate cancer. *Cancer Res.* 67:6130–6135.

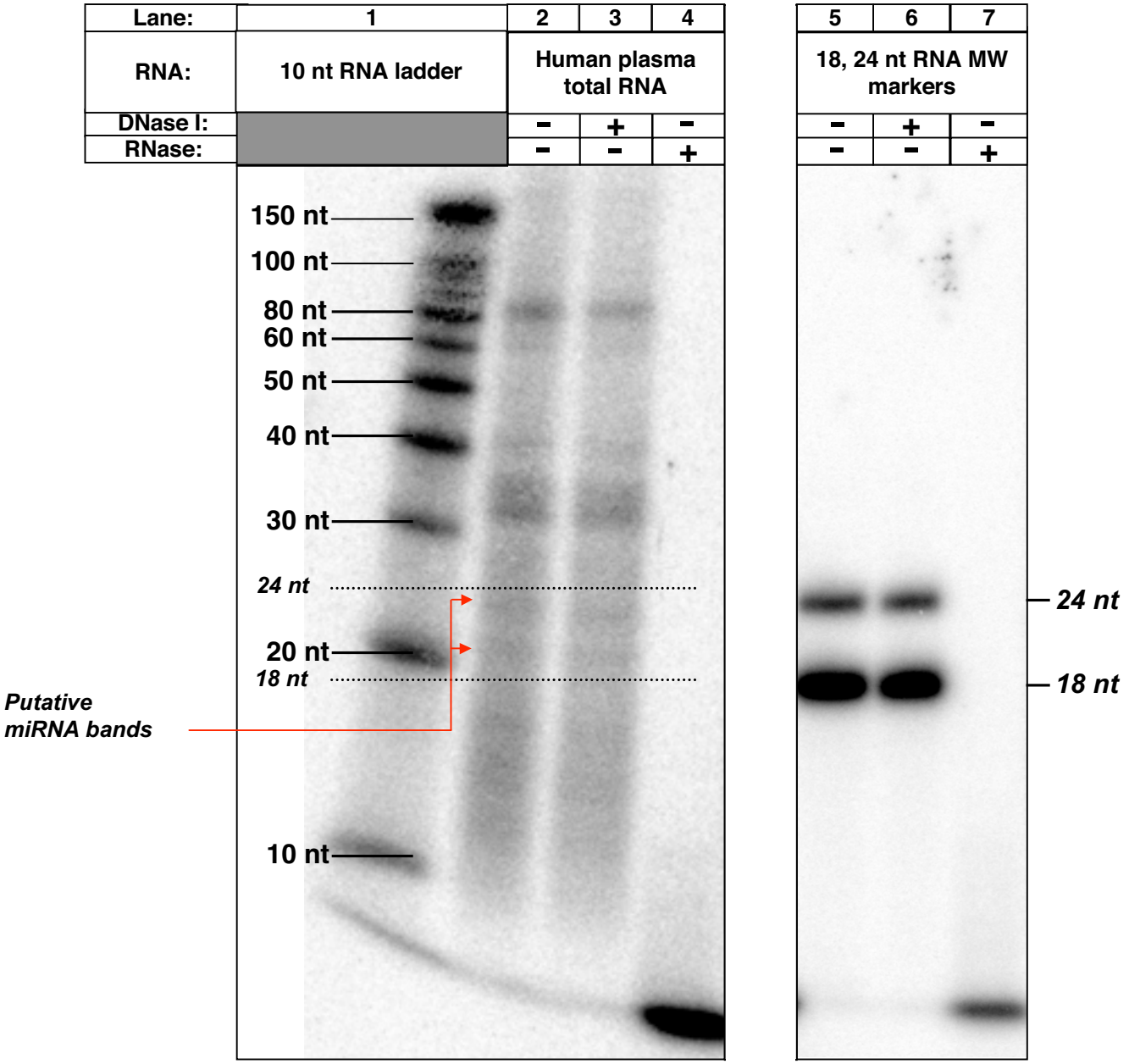

Fig. S1. Human plasma contains small RNA of size typical of miRNAs. Lanes 2–4 represent 100 ng of human plasma total RNA (from individual 006 described in Table S6) treated with calf intestinal phosphatase followed by labeling of accessible 5′ hydroxyl groups with $\gamma[^{32}]$ATP using T4 polynucleotide kinase. The radiolabeled material was either left untreated (lane 2), treated with DNase I (lane 3), or treated with RNase (lane 4) (Roche 1119915) before denaturing gel electrophoresis (15% polyacrylamide gel) and phosphorimaging. Samples were run alongside a 10 nt RNA ladder (lane 1; labels and solid lines indicate molecular size of each band of the ladder). Synthetic 18- and 24-nt markers (18 nt: AGCGUGUAGGGAUCCAAA, 24 nt: GGCCAACGUUCUCAACAAUAGUGA) (Dharmacon) were also run in parallel, three lanes away on the same gel (to avoid cross-contamination) and were subjected to the same conditions as the plasma RNA samples (lanes 5–7). Dotted lines in the human plasma lanes (based on the synthetic miRNAs in lanes 5 and 6) define the 18- to 24-nt size range, which encompasses the size range of known human miRNAs. All detected RNA was of low molecular weight (i.e., migrating at sizes $<$100 nt). Two bands were detected in the 18- to 24-nt size range (indicated by the red arrows). One was observed at $\sim$22 nt (which is the most common length for known miRNAs) and the other just below the 24-nt marker, which is still within the size range of many known miRNAs.

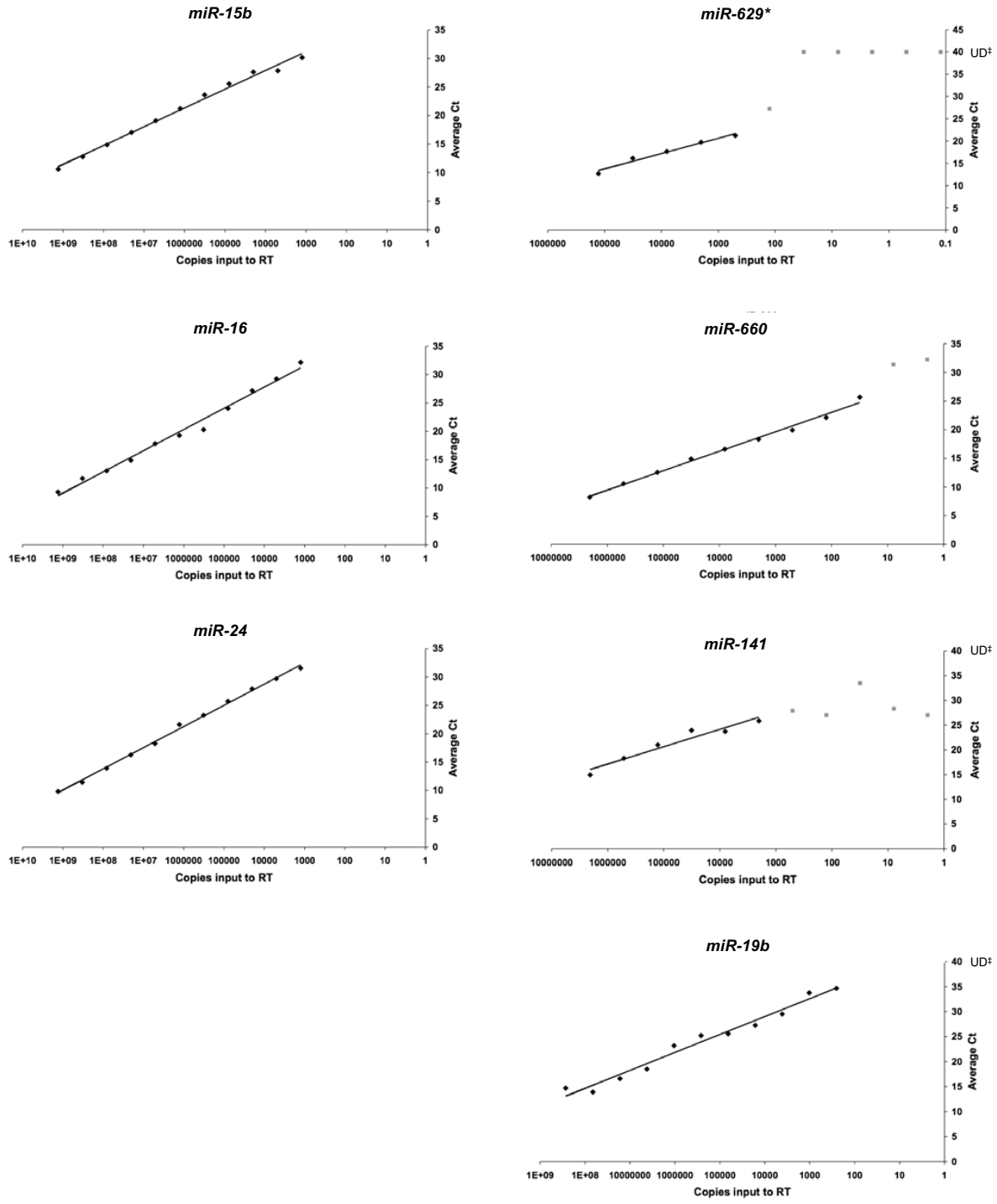

Fig. S2. Standard curves for TaqMan qRT-PCR assays used in this study. Standard curves were generated for each miRNA assay using a dilution series of known input amounts of synthetic miRNA oligonucleotide corresponding to the target of the assay (Table S5). The dilution series samples were run using common RT and PCR enzyme master mixes and on the same plate as experimental samples. In cases where standard curves were run on several plates (for several different experiments), only a representative standard curve is shown. Data points in gray are those for which the measured Ct was interpreted to be below the linear range of the assay, and were not used for derivation of the trend line. UD denotes data points that were undetermined (i.e., no significant amplification signal was discernable); these were arbitrarily set to a Ct of 40 for display on the graph.

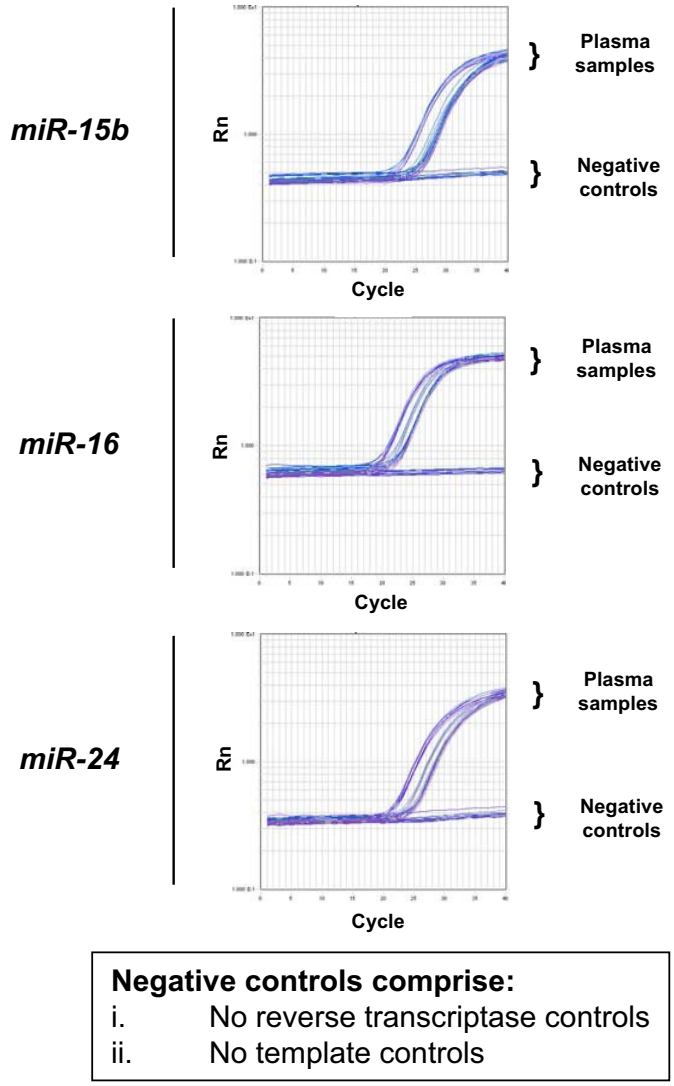

Fig. S3. Real-time PCR amplification plots for *miR-15b*, *miR-16*, and *miR-24* measured in human plasma samples from three individuals. Each graph represents amplification [presented on the *y*-axis as Rn: the fluorescence emission intensity of the reporter dye (FAM) normalized to the passive reference dye (ROX)] plotted against cycle number (presented on the *x*-axis as the cycle at which fluorescence was detected above an automatically determined threshold) for the indicated miRNA from plasma RNA isolated from three individuals. The curves represent technical replicates (in triplicate) of real-time PCR for the RNA sample from each individual. The negative control curves represent technical replicates of no template controls and reverse transcriptase negative controls corresponding to each sample. Lack of amplification in the reverse transcriptase negative controls confirms that amplification signal in the plasma RNA qRT-PCR samples is derived from an RNA template (rather than from genomic DNA contamination).

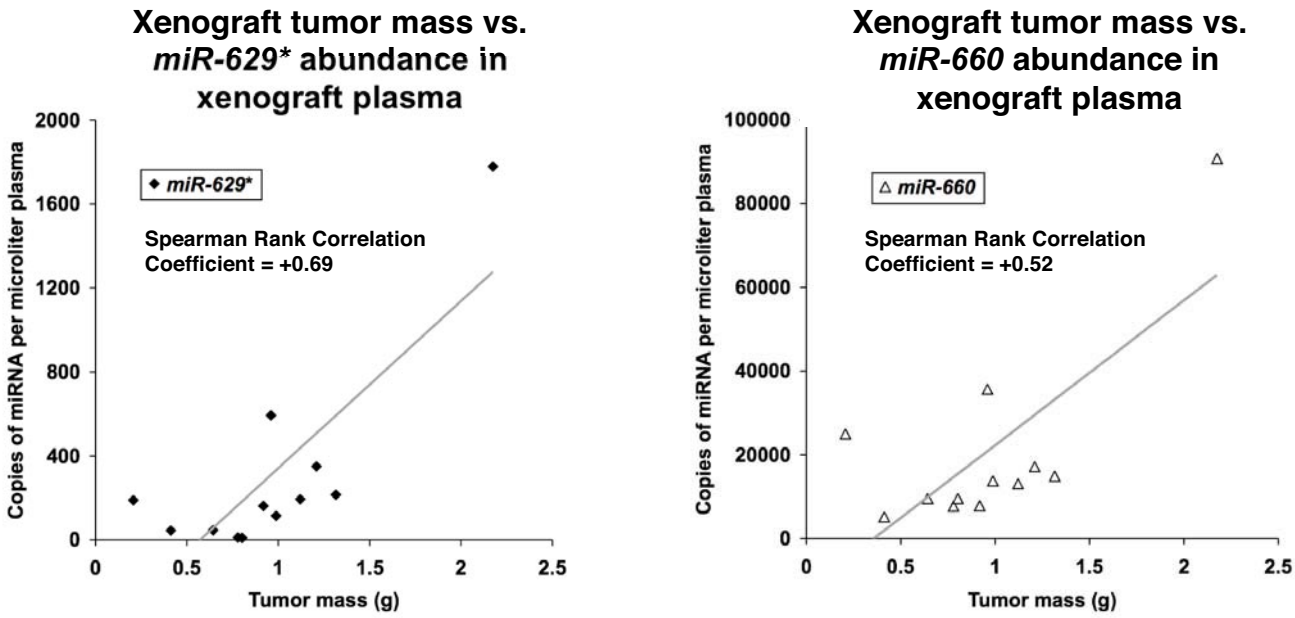

Fig. S4. Abundance of tumor-derived miRNAs in plasma of xenografted mice correlates with tumor mass. The abundance of tumor-derived miRNAs *miR-629** (*Left*) and *miR-660* (*Right*) in the plasma of 12 mice xenografted with 22Rv1 prostate cancer cells is plotted against the mass of the corresponding primary tumor. The blood used for plasma isolation and miRNA measurement was drawn immediately before death of the mouse and recovery of the tumor. Levels of both miRNAs were moderately correlated with tumor mass (*miR-629**: Spearman Rank Correlation Coefficient = +0.69; *miR-660*: Spearman Rank Correlation Coefficient = +0.52).

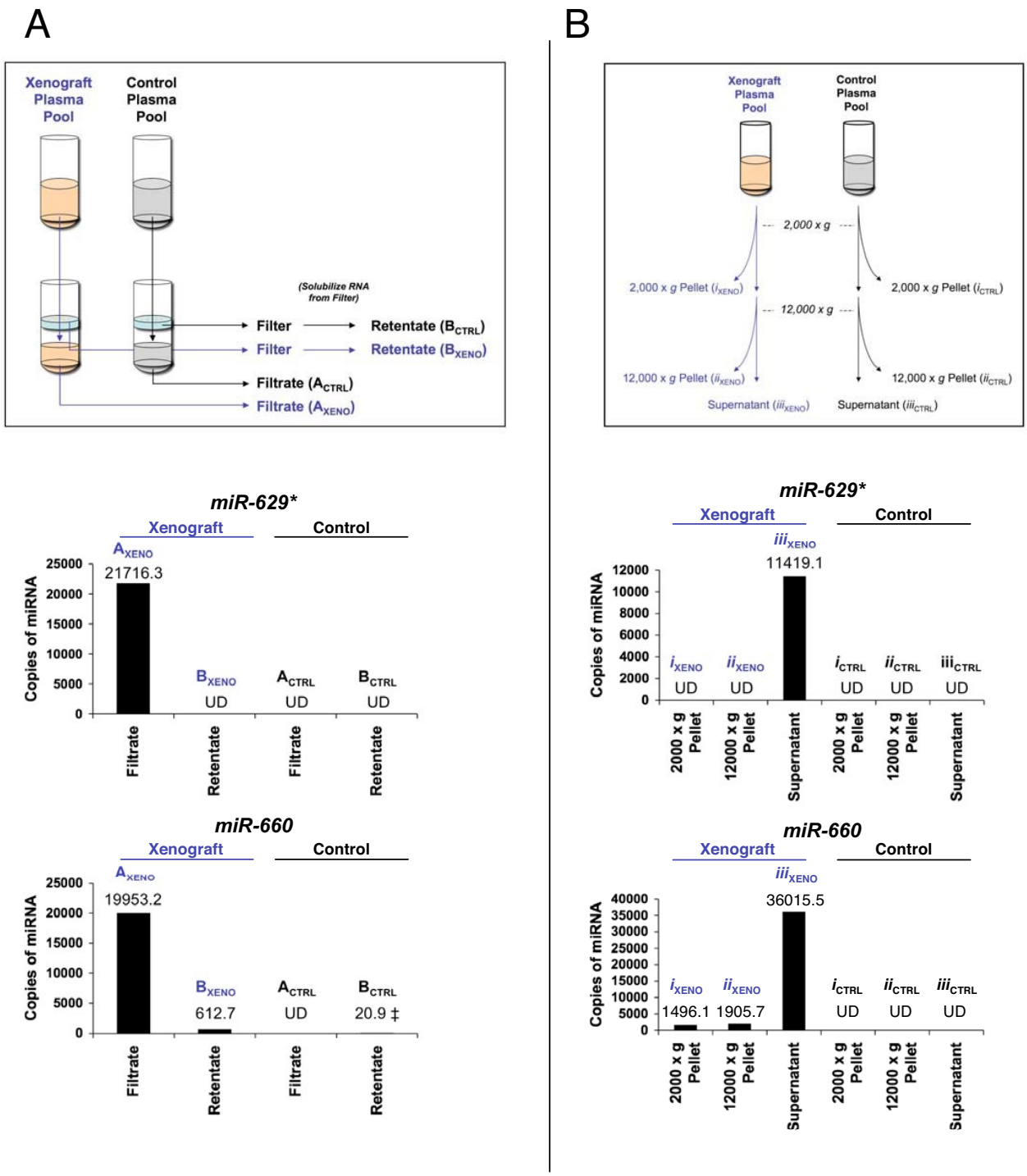

Fig. S5. (*A*) Tumor-derived miRNAs in plasma pass through a 0.22-μm filter. The diagram depicts the experimental schema for plasma filtration. The graphs display the total number of copies of the tumor-derived miRNAs *miR-629** and *miR-660* recovered from the indicated samples. Numbers provided above sample labels or bars indicate the experimental value for number of copies of a given miRNA. UD indicates that the miRNA was undetectable in a given sample. As expected, *miR-629** and *miR-660* were largely undetectable in plasma from the control (nontumor-bearing) animals. The retentate sample from the control group (i.e., sample B_{CTRL}) formally yielded a value of 20.9 copies; however, the Ct value was below the linear range of accurate quantification based on the standard curve and likely represents low-level background amplification. (*B*) Tumor-derived miRNAs in plasma are not pelleted by additional 2000 $\times$ *g* or 12,000 $\times$ *g* centrifugations. The diagram depicts the experimental schema for plasma differential centrifugation. The graphical display of results is presented as described for *A*. As expected, *miR-629** and *miR-660* were undetectable in plasma from the control (nontumor-bearing) animals.

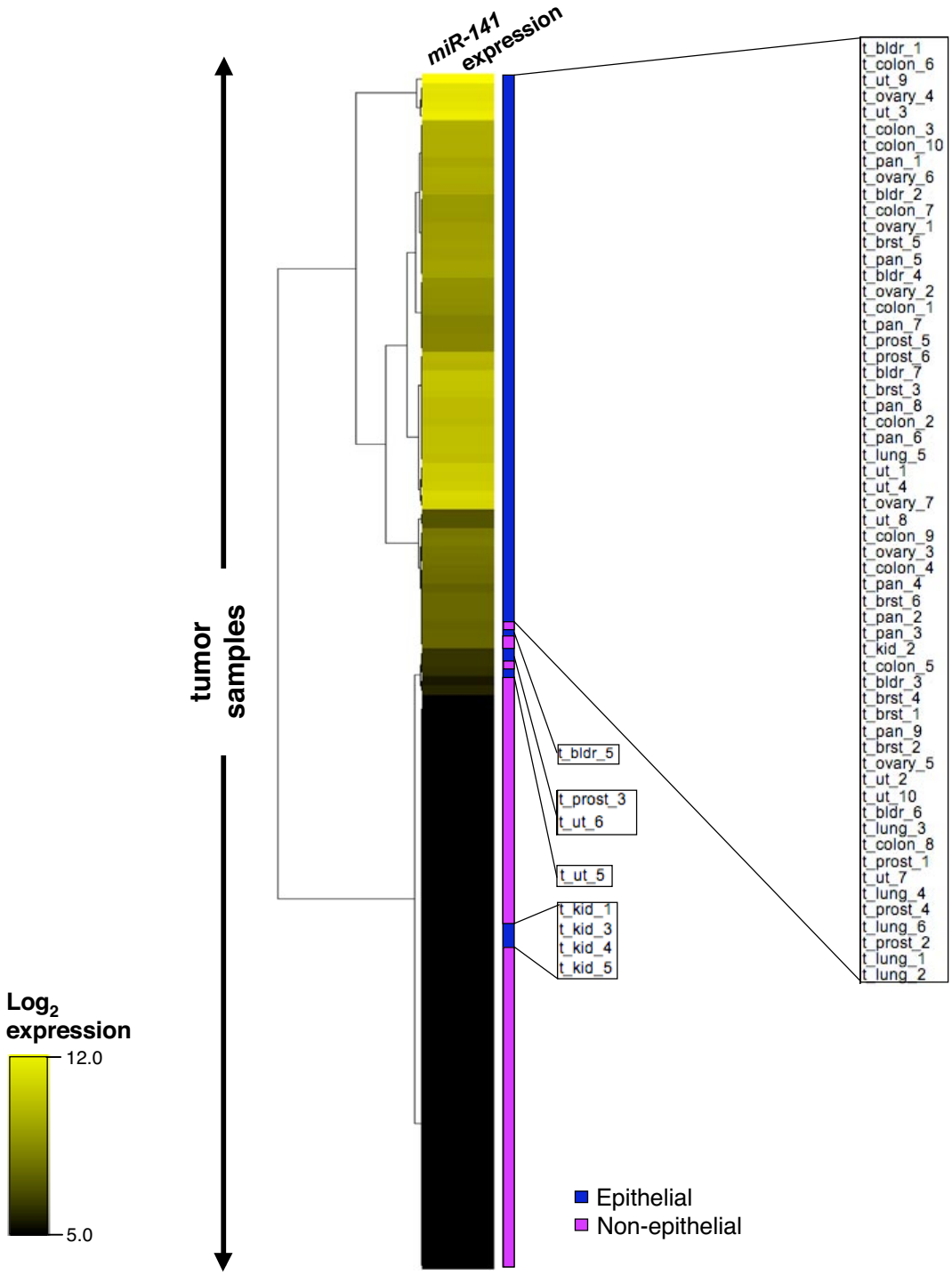

Fig. S6. *miR-141* is expressed in an epithelial-restricted pattern in a broad range of human cancers based on analysis of the Lu *et al.* (1) human cancer miRNA profiling dataset. The heatmap depicts $\log_2$ expression values of *miR-141* across the range of human tumor samples present in the dataset (see *SI Text* for more details). Samples are classified as epithelial (blue) or non-epithelial (purple) based on the designations of Lu *et al.* The four kidney cancers, although specified as epithelial in the Lu *et al.* dataset, could show features of nonepithelial differentiation, as most renal cell carcinomas are of the clear cell histologic subtype and have been shown previously to lose expression of the epithelial cell adhesion molecule (EpCAM) (2). We speculate that this may explain the absence of *miR-141* expression in the kidney cancers in the study by Lu *et al.*

1. Lu J, *et al.* (2005) MicroRNA expression profiles classify human cancers. *Nature* 435:834–838.
2. Seligson DB, *et al.* (2004) Epithelial cell adhesion molecule (KSA) expression: Pathobiology and its role as an independent predictor of survival in renal cell carcinoma. *Clin Cancer Res* 10:2659–2669.

Table 1. Results of TaqMan Low-Density Array qRT-PCR profiling of 22Rv1 cells

Detector	Ct	Mouse homolog?
hsa-miR-200c-4373096	20.843742	Yes
hsa-miR-16–4373121	21.008804	Yes
hsa-miR-93–4373012	21.778013	Yes
hsa-miR-19b-4373098	22.088984	Yes
hsa-miR-26a-4373070	22.283915	Yes
hsa-miR-92a-4373013	22.588377	Yes
hsa-miR-20a-4373286	22.745483	Yes
hsa-let-7b-4373168	22.75965	Yes
hsa-miR-106b-4373155	23.09081	Yes
hsa-miR-24–4373072	23.12045	Yes
hsa-miR-26b-4373069	23.224205	Yes
hsa-miR-594–4380958	23.552273	N/A - later found to be a tRNA fragment
hsa-miR-191–4373109	23.600554	Yes
hsa-miR-484–4381032	23.930113	Yes
hsa-miR-375–4373027	24.112288	Yes
hsa-miR-25–4373071	24.178068	Yes
hsa-miR-15b-4373122	24.24048	Yes
hsa-miR-30c-4373060	24.33494	Yes
hsa-miR-132–4373143	24.447603	Yes
hsa-miR-19a-4373099	24.5984	Yes
hsa-miR-30b-4373290	24.808388	Yes
hsa-miR-125a-4373149	24.909286	Yes
hsa-miR-331–4373046	24.919724	Yes
hsa-miR-141–4373137	25.243183	Yes
hsa-let-7a-4373169	25.280457	Yes
hsa-miR-27a-4373287	25.294226	Yes
hsa-miR-195–4373105	25.487253	Yes
hsa-miR-30a-5p-4373061	25.62212	Yes
hsa-miR-186–4373112	25.659605	Yes
hsa-miR-320–4373055	25.705463	Yes
hsa-miR-148a-4373130	25.887983	Yes
hsa-miR-17–5p-4373119	25.972061	Yes
hsa-let-7 g-4373163	26.000093	Yes
hsa-miR-30d-4373059	26.014767	Yes
hsa-miR-103–4373158	26.05778	Yes
hsa-miR-21–4373090	26.123838	Yes
hsa-miR-425–5p-4380926	26.16638	Yes
hsa-miR-301a-4373064	26.218494	Yes
hsa-miR-9–4373285	26.228582	Yes
hsa-miR-374a-4373028	26.262016	Yes
hsa-miR-197–4373102	26.407486	Yes
hsa-miR-130b-4373144	26.559368	Yes
hsa-miR-565–4380942	26.597208	N/A - later found to be a tRNA fragment
hsa-miR-10a-4373153	26.612278	Yes
hsa-miR-196a-4373104	26.6339	Yes
hsa-miR-324–3p-4373053	26.643904	Yes
hsa-miR-140–4373138	26.651573	Yes
hsa-miR-182–4373271	26.679113	Yes
hsa-miR-383–4373018	26.68571	Yes
hsa-miR-149–4373128	26.835257	Yes
hsa-miR-615–4380991	26.942888	Yes
hsa-miR-148b-4373129	27.010065	Yes
hsa-miR-125b-4373148	27.18106	Yes
hsa-miR-345–4373039	27.20657	Yes
hsa-miR-335–4373045	27.227848	Yes
hsa-miR-7–4373014	27.235477	Yes
hsa-let-7c-4373167	27.256641	Yes
hsa-miR-31–4373190	27.268515	Yes
hsa-miR-660–4380925	**27.309317**	**No**
hsa-miR-423–4373015	27.413136	Yes
hsa-miR-20b-4373263	27.531952	Yes
hsa-miR-151–4373179	27.60408	Yes
hsa-miR-100–4373160	27.697943	Yes
hsa-miR-324–5p-4373052	27.72548	Yes

Detector	Ct	Mouse homolog?
hsa-miR-29a-4373065	27.74265	Yes
hsa-miR-532–4380928	27.765844	Yes
hsa-miR-342–4373040	27.794342	Yes
hsa-miR-224–4373187	27.842451	Yes
hsa-miR-137–4373174	27.852215	Yes
hsa-miR-28–4373067	27.936628	Yes
hsa-miR-30a-3p-4373062	27.945545	Yes
hsa-miR-30e-3p-4373057	27.96953	Yes
hsa-miR-29c-4373289	27.99324	Yes
hsa-miR-27b-4373068	28.023924	Yes
hsa-miR-203–4373095	28.182741	Yes
hsa-let-7f-4373164	28.203585	Yes
hsa-miR-99b-4373007	28.219166	Yes
hsa-miR-181b-4373116	28.323942	Yes
hsa-miR-328–4373049	28.46557	Yes
hsa-miR-99a-4373008	28.475124	Yes
hsa-miR-15a-4373123	28.519396	Yes
hsa-miR-361–4373035	28.542204	Yes
hsa-miR-181d-4373180	28.671408	Yes
hsa-miR-9*-4378074	28.699503	Yes
hsa-miR-210–4373089	28.701073	Yes
hsa-miR-18a-4373118	28.722933	Yes
hsa-miR-135a-4373140	28.735958	Yes
hsa-miR-362–4378092	28.758781	Yes
hsa-miR-183–4373114	28.825584	Yes
hsa-miR-365–4373194	28.891764	Yes
hsa-miR-146b-4373178	28.923525	Yes
hsa-let-7d-4373166	29.013346	Yes
hsa-miR-192–4373108	29.060951	Yes
hsa-miR-425–4373202	29.104452	Yes
hsa-miR-152–4373126	29.110943	Yes
hsa-miR-378–4373024	29.159906	Yes
hsa-miR-98–4373009	29.177269	Yes
hsa-miR-101–4373159	29.2103	Yes
hsa-miR-23b-4373073	29.24969	Yes
hsa-miR-187–4373111	29.379126	Yes
hsa-miR-196b-4373103	29.408249	Yes
hsa-miR-497–4373222	29.532091	Yes
hsa-miR-218–4373081	29.553488	Yes
hsa-miR-32–4373056	29.556976	Yes
hsa-miR-501–4373226	29.55937	Yes
hsa-miR-194–4373106	29.714993	Yes
hsa-miR-452*-4378077	29.761187	No
hsa-miR-22–4373079	29.847921	Yes
hsa-miR-200a-4378069	30.003298	Yes
hsa-miR-629–4380969	**30.080704**	**No**
hsa-miR-135b-4373139	30.168968	Yes
hsa-miR-23a-4373074	30.206684	Yes
hsa-miR-340–4373041	30.288404	Yes
hsa-miR-155–4373124	30.64169	Yes
hsa-miR-200b-4381028	30.759663	Yes
hsa-miR-597–4380960	30.817492	No
hsa-miR-491–4373216	30.829758	Yes
hsa-miR-330–4373047	31.041233	Yes
hsa-miR-339–4373042	31.117188	Yes
hsa-miR-550–4380954	31.147772	No
hsa-miR-222–4373076	31.252699	Yes
hsa-miR-30e-5p-4373058	31.28834	Yes
hsa-miR-193a-4373107	31.339767	Yes
hsa-miR-10b-4373152	31.389738	Yes
hsa-miR-486–4378096	31.448664	Yes
hsa-miR-126–4378064	31.58067	Yes
hsa-miR-107–4373154	31.621546	Yes
hsa-let-7e-4373165	31.669636	Yes
hsa-miR-17–3p-4373120	31.723549	Yes

Detector	Ct	Mouse homolog?
hsa-miR-548d-4381008	31.81656	No
hsa-miR-500–4373225	31.886179	Yes
hsa-miR-449a-4373207	32.123947	Yes
hsa-miR-642–4380995	32.219257	No
hsa-miR-616–4380992	32.286846	No
hsa-miR-429–4373203	32.462257	Yes
hsa-miR-213–4373086	32.498528	Yes
hsa-miR-509–4373234	32.52028	Yes
hsa-miR-650–4381006	32.52341	No
hsa-miR-130a-4373145	32.810963	Yes
hsa-miR-618–4380996	33.05673	No
hsa-miR-579–4381023	33.15031	No
hsa-miR-545–4380918	33.151085	No
hsa-miR-422a-4373200	33.26565	No
hsa-miR-490–4373215	33.30832	Yes
hsa-miR-449b-4381011	33.393772	Yes
hsa-miR-105–4373157	33.459824	Yes
hsa-miR-622–4380961	33.527863	No
hsa-miR-95–4373011	33.590992	No
hsa-miR-452–4373281	33.60625	Yes
hsa-miR-542–5p-4378105	33.620365	Yes
hsa-miR-424–4373201	33.830677	Yes
hsa-miR-589–4380953	33.951397	No
hsa-miR-204–4373094	33.953087	Yes
hsa-miR-572–4381017	33.989155	No
hsa-miR-502–4373227	34.142883	No
hsa-miR-551a-4380929	34.18227	No
hsa-miR-139–4373176	34.18969	Yes
RNU6B-4373381	34.197094	N/A - a snoRNA
hsa-miR-659–4380924	34.333885	No
hsa-miR-34a-4373278	34.335876	Yes
hsa-miR-199a*-4378068	34.35002	Yes
hsa-miR-576–4381021	34.364895	Yes
hsa-miR-219–4373080	34.37666	Yes
hsa-miR-489–4373214	34.544186	Yes
hsa-miR-601–4380965	34.77672	No
hsa-miR-548c-4380993	34.893776	No
hsa-miR-580–4381024	34.9058	No
hsa-miR-520d-4373254	35.041225	No
hsa-miR-126*-4373269	35.08921	Yes
hsa-miR-96–4373010	35.45431	Yes
hsa-miR-515–3p-4373241	35.585583	No
hsa-miR-181c-4373115	35.639126	Yes
hsa-miR-504–4373229	35.7073	Yes
hsa-miR-422b-4373016	35.73341	Yes
hsa-miR-142–3p-4373136	35.883354	Yes
hsa-miR-127–4373147	36.043385	Yes
hsa-miR-518f-4378083	36.156406	No
hsa-miR-627–4380967	36.448597	No
hsa-miR-189–4378067	36.58372	Yes
hsa-miR-514–4373240	36.68456	No
hsa-miR-432*-4378076	36.841095	No
hsa-miR-630–4380970	37.480858	No
hsa-miR-518b-4373246	37.488377	No
hsa-miR-517b-4373244	37.707623	No
hsa-miR-596–4380959	37.80205	No
hsa-miR-518e-4373265	37.973427	No
hsa-miR-586–4380949	38.028755	No
hsa-miR-302c*-4373277	38.14734	Yes
hsa-miR-190–4373110	38.190205	Yes
hsa-miR-146a-4373132	38.309822	Yes
hsa-miR-552–4380930	38.393467	No
hsa-miR-652–4380927	38.717022	Yes
hsa-miR-517a-4373243	38.790215	No
hsa-miR-646–4381002	38.79356	No

Detector	Ct	Mouse homolog?
hsa-miR-185–4373181	38.79913	Yes
hsa-miR-553–4380931	39.17754	No
hsa-miR-548b-4380951	39.343506	No
hsa-miR-214–4373085	39.497402	Yes
hsa-miR-34b-4373037	Undetermined	
hsa-miR-34c-4373036	Undetermined	
hsa-miR-142–5p-4373135	Undetermined	
hsa-miR-215–4373084	Undetermined	
hsa-miR-221–4373077	Undetermined	
hsa-miR-223–4373075	Undetermined	
hsa-miR-372–4373029	Undetermined	
hsa-miR-200a-4373273	Undetermined	
hsa-miR-1–4373161	Undetermined	
hsa-miR-296–4373066	Undetermined	
hsa-miR-302a-4373275	Undetermined	
hsa-miR-302d-4373063	Undetermined	
hsa-miR-367–4373034	Undetermined	
hsa-miR-369–5p-4373195	Undetermined	
hsa-miR-510–4373235	Undetermined	
hsa-miR-511–4373236	Undetermined	
hsa-miR-515–5p-4373242	Undetermined	
hsa-miR-517c-4373264	Undetermined	
hsa-miR-518a-4373186	Undetermined	
hsa-miR-518c-4373247	Undetermined	
hsa-miR-518d-4373248	Undetermined	
hsa-miR-520a-4373268	Undetermined	
hsa-miR-520b-4373252	Undetermined	
hsa-miR-520c-4373253	Undetermined	
hsa-miR-520e-4373255	Undetermined	
hsa-miR-520f-4373256	Undetermined	
hsa-miR-520 g-4373257	Undetermined	
hsa-miR-520 h-4373258	Undetermined	
hsa-miR-133a-4373142	Undetermined	
hsa-miR-184–4373113	Undetermined	
hsa-miR-206–4373092	Undetermined	
hsa-miR-211–4373088	Undetermined	
hsa-miR-216–4373083	Undetermined	
hsa-miR-217–4373082	Undetermined	
hsa-miR-371–4373030	Undetermined	
hsa-miR-379–4373023	Undetermined	
hsa-miR-381–4373020	Undetermined	
hsa-miR-198–4373101	Undetermined	
hsa-miR-133b-4373172	Undetermined	
hsa-miR-299–5p-4373188	Undetermined	
hsa-miR-409–5p-4373197	Undetermined	
hsa-miR-432–4373280	Undetermined	
hsa-miR-433–4373205	Undetermined	
hsa-miR-485–5p-4373212	Undetermined	
hsa-miR-494–4373219	Undetermined	
hsa-miR-506–4373231	Undetermined	
hsa-miR-508–4373233	Undetermined	
hsa-miR-521–4373259	Undetermined	
hsa-miR-134–4373141	Undetermined	
hsa-miR-147–4373131	Undetermined	
hsa-miR-153–4373125	Undetermined	
hsa-miR-205–4373093	Undetermined	
hsa-miR-208–4373091	Undetermined	
hsa-miR-220–4373078	Undetermined	
hsa-miR-325–4373051	Undetermined	
hsa-miR-326–4373050	Undetermined	
hsa-miR-337–4373044	Undetermined	
hsa-miR-380–3p-4373022	Undetermined	
hsa-miR-193b-4373185	Undetermined	
hsa-miR-496–4373221	Undetermined	
hsa-miR-122a-4373151	Undetermined	

Detector	Ct	Mouse homolog?
hsa-miR-124a-4373150	Undetermined	
hsa-miR-128b-4373170	Undetermined	
hsa-miR-129–4373171	Undetermined	
hsa-miR-143–4373134	Undetermined	
hsa-miR-145–4373133	Undetermined	
hsa-miR-182–4378066	Undetermined	
hsa-miR-18b-4373184	Undetermined	
hsa-miR-202–4378075	Undetermined	
hsa-miR-202–4373274	Undetermined	
hsa-miR-299–3p-4373189	Undetermined	
hsa-miR-302a-4378070	Undetermined	
hsa-miR-302b-4378071	Undetermined	
hsa-miR-302b-4373276	Undetermined	
hsa-miR-302c-4378072	Undetermined	
hsa-miR-329–4373191	Undetermined	
hsa-miR-33–4373048	Undetermined	
hsa-miR-369–3p-4373032	Undetermined	
hsa-miR-376a-4373026	Undetermined	
hsa-miR-376b-4373196	Undetermined	
hsa-miR-380–5p-4373021	Undetermined	
hsa-miR-410–4378093	Undetermined	
hsa-miR-412–4373199	Undetermined	
hsa-miR-512–5p-4373238	Undetermined	
hsa-miR-199a-4373272	Undetermined	
hsa-miR-199b-4373100	Undetermined	
hsa-miR-323–4373054	Undetermined	
hsa-miR-338–4373043	Undetermined	
hsa-miR-368–4373033	Undetermined	
hsa-miR-373–4378073	Undetermined	
hsa-miR-373–4373279	Undetermined	
hsa-miR-382–4373019	Undetermined	
hsa-miR-448–4373206	Undetermined	
hsa-miR-450–4373208	Undetermined	
hsa-miR-451–4373209	Undetermined	
hsa-miR-453–4373210	Undetermined	
hsa-miR-485–3p-4378095	Undetermined	
hsa-miR-488–4373213	Undetermined	
hsa-miR-492–4373217	Undetermined	
hsa-miR-493–4373218	Undetermined	
hsa-miR-503–4373228	Undetermined	
hsa-miR-505–4373230	Undetermined	
hsa-miR-507–4373232	Undetermined	
hsa-miR-513–4373239	Undetermined	
hsa-miR-516–5p-4378099	Undetermined	
hsa-miR-517–4378078	Undetermined	
4343438-Blank	Undetermined	
hsa-miR-518c-4378082	Undetermined	
hsa-miR-519b-4373250	Undetermined	
hsa-miR-519c-4373251	Undetermined	
hsa-miR-519d-4373266	Undetermined	
hsa-miR-519e-4373267	Undetermined	
hsa-miR-522–4373245	Undetermined	
hsa-miR-523–4373260	Undetermined	
hsa-miR-524–4378087	Undetermined	
hsa-miR-526b-4378080	Undetermined	
hsa-miR-651–4381007	Undetermined	
hsa-miR-376a-4378104	Undetermined	
hsa-miR-544–4380919	Undetermined	
hsa-miR-656–4380920	Undetermined	
hsa-miR-549–4380921	Undetermined	
hsa-miR-657–4380922	Undetermined	
hsa-miR-658–4380923	Undetermined	
hsa-miR-554–4380932	Undetermined	
hsa-miR-555–4380933	Undetermined	
hsa-miR-562–4380939	Undetermined	

Detector	Ct	Mouse homolog?
hsa-miR-563–4380940	Undetermined	
hsa-miR-564–4380941	Undetermined	
hsa-miR-566–4380943	Undetermined	
hsa-miR-551b-4380945	Undetermined	
hsa-miR-569–4380946	Undetermined	
hsa-miR-570–4380947	Undetermined	
hsa-miR-548a-4380948	Undetermined	
hsa-miR-587–4380950	Undetermined	
hsa-miR-588–4380952	Undetermined	
hsa-miR-591–4380955	Undetermined	
hsa-miR-593–4380957	Undetermined	
hsa-miR-599–4380962	Undetermined	
hsa-miR-600–4380963	Undetermined	
hsa-miR-624–4380964	Undetermined	
hsa-miR-626–4380966	Undetermined	
hsa-miR-639–4380987	Undetermined	
hsa-miR-613–4380989	Undetermined	
hsa-miR-614–4380990	Undetermined	
hsa-miR-617–4380994	Undetermined	
hsa-miR-644–4380999	Undetermined	
hsa-miR-647–4381003	Undetermined	
hsa-miR-649–4381005	Undetermined	
hsa-miR-661–4381009	Undetermined	
hsa-miR-662–4381010	Undetermined	
hsa-miR-653–4381012	Undetermined	
hsa-miR-411–4381013	Undetermined	
hsa-miR-654–4381014	Undetermined	
4343438-Blank	Undetermined	
hsa-miR-575–4381020	Undetermined	
hsa-miR-578–4381022	Undetermined	
hsa-miR-585–4381027	Undetermined	
hsa-miR-512–3p-4381034	Undetermined	
hsa-miR-631–4380971	Undetermined	
hsa-miR-363–4380917	Undetermined	
hsa-miR-487b-4378102	Undetermined	
hsa-miR-645–4381000	Undetermined	
hsa-miR-556–4380934	Undetermined	
hsa-miR-558–4380936	Undetermined	
hsa-miR-603–4380972	Undetermined	
hsa-miR-606–4380974	Undetermined	
hsa-miR-607–4380975	Undetermined	
hsa-miR-608–4380976	Undetermined	
hsa-miR-609–4380978	Undetermined	
hsa-miR-633–4380979	Undetermined	

Assay results for *miR-660* and *miR-629** are indicated by bold text. Note that miRNA names and assay numbers provided are from the *Taq*Man TLDA qRT-PCR card literature, which uses miRNA nomenclature that predates the current miRBase release (v.10.1). Of particular note, *miR-629** as referenced throughout this article is actually listed as a *miR-629* assay in Applied Biosystems TaqMan literature because this miRNA had its name changed from *miR-629* to *miR-629** between earlier and more recent versions of miRBase. Cycle threshold (Ct) values obtained from qRT-PCR analysis of each miRNA are shown.Yes, No: human miRNAs with homology in mouse are noted. N/A indicates non-miRNA Taqman assays

Table 2. Results of screening miRNA biomarker candidates by qRT-PCR in serum pools prepared from 25 normal control individuals and 25 patients with advanced prostate cancer

	Normal controls serum group		Prostate cancer patients serum group			Relative quantification: prostate cancer serum/normal serum
miRNA	Raw Ct	Δ Ct	Raw Ct	Δ Ct	ΔΔ Ct	RQ
miR-100	21.8918235	5.899684833	21.0723035	4.431417167	−1.468267667	2.77
miR-125b	22.940055	6.947916333	20.922019	4.281132667	−2.666783667	6.35
miR-141	**25.4960765**	**9.503937833**	**20.631195**	**3.990308667**	**−5.513629167**	**45.68**
miR-143	23.0193355	7.027196833	23.064886	6.423999667	−0.603197167	1.52
miR-205	NQ	NQ	NQ	NQ	NQ	NQ
miR-296	22.9490635	6.38040225	22.3942595	5.82559825	−0.554804	1.47

miRNA expression is represented as raw cycle threshold (Ct) values from qRT-PCR analysis (using SDS software v.2.2.2). Note that cycle threshold values are inversely related to expression level (e.g. a lower Ct value corresponds to higher expression). Delta Ct (ΔCt) values are defined as the Raw Ct value − Avg Ct of spiked-in synthetic *C. elegans* miRNAs for that sample. Additional details about the use of the spiked-in normalization controls are provided in *SI Text*. Relative quantification (RQ) reflects the ratio of expression in the cancer pool relative to the control pool and is calculated as $2^{(-\Delta\Delta Ct)}$ where ΔΔCt is defined as the $\Delta Ct_{Cancer} - \Delta Ct_{Control}$. *miR-141* was the most highly overrepresented miRNA in prostate cancer serum among the miRNAs in this group and is highlighted in boldface type. NQ = not quantifiable; in the case of *miR-205* the level of expression of the miRNA was below the limit of quantitation of the assay in both the control and cancer serum pools.

Table 3. Clinical data associated with serum samples corresponding to human prostate cancer patients and healthy control individuals (all males)

Sample ID no.	Sample class	Age of individual at time of sample collection, years	Year of sample collection	Normalized copies of *miR-141* per microliter serum	PSA
17592M	Normal	57	1999	417.9	0.76
17677C	Normal	72	1999	1771.9	0.58
17681C	Normal	65	1999	788.7	0.68
17837G	Normal	77	1999	731.4	0.50
18510G	Normal	75	1999	414.4	1.03
18643J	Normal	64	2000	169.7	0.89
19279G	Normal	56	1998	145.5	0.92
19490H	Normal	59	1999	1459.3	0.79
19512A	Normal	79	1999	69.3	0.56
19538E	Normal	52	1997	215.3	0.42
20428J	Normal	69	2002	615.4	0.20
20487G	Normal	52	1999	621.3	0.42
20511M	Normal	67	2000	83.5	0.20
20548D	Normal	53	1999	373.9	0.90
20680H	Normal	50	1999	292.5	0.31
20690H	Normal	58	1999	468.8	0.93
21087N	Normal	65	1999	603.9	0.32
21088P	Normal	67	2003	113.2	0.73
21096G	Normal	51	1999	201.4	0.92
21105H	Normal	71	1999	445.5	1.03
21116W	Normal	60	1999	308.2	0.35
21316C	Normal	56	1999	598.5	1.08
21335C	Normal	54	1999	252.0	0.86
21353C	Normal	52	2000	2508.6	0.54
21488S	Normal	55	2000	361.3	0.65
12801M	Prostate cancer	72	2002	833.2	11.48
12872M	Prostate cancer	63	2001	78639.3	8420
13394W	Prostate cancer	85	2002	1031.9	9.17
16501R	Prostate cancer	70	2001	476.4	45.16
17330O	Prostate cancer	53	2000	75267.9	5974
18006M	Prostate cancer	70	2000	9309.6	345.9
18458T	Prostate cancer	73	1998	224.9	171.8
18528G	Prostate cancer	81	2002	574.9	4.66
19385L	Prostate cancer	64	2003	937.2	2.54
19399M	Prostate cancer	77	1999	89811.2	3647.4
19597W	Prostate cancer	47	2000	761.6	215.4
19598G	Prostate cancer	84	1999	5505.7	37.35
20445C	Prostate cancer	74	1998	20585.2	2151
20748C	Prostate cancer	57	1999	5004.9	23.04
20773L	Prostate cancer	72	2002	2985.2	680.3
20847U	Prostate cancer	84	1999	521.7	46.78
20937H	Prostate cancer	63	1999	7493.1	432
20952H	Prostate cancer	60	2000	11113.9	912.5
21433C	Prostate cancer	65	2003	3404.8	963.4
22557O	Prostate cancer	67	2005	12055.9	500.9
22576C	Prostate cancer	64	2003	46125.8	38.14
23187D	Prostate cancer	61	2004	1503.4	1.57
23210H	Prostate cancer	59	2005	866.5	170.64
23517S	Prostate cancer	68	2005	4453.9	34.07
23552H	Prostate cancer	72	2005	11727.3	1272.4

Table 4. Results of massively parallel sequencing (i.e., 454 sequencing) of small RNA cDNA libraries from human primary prostate epithelial cell (PEC) or primary stromal cell (PSC) cultures

miRNA	No. of reads in PEC	Fraction of reads in PEC	No. of reads in PSC	Fraction of reads in PSC	Ratio: fraction of reads in PEC/fraction of Reads in PSC	Fisher's Exact Test *P*
hsa-miR-200b	**49**	**8.11E-04**	**0**		∞	**<1E-6**
hsa-miR-141	**35**	**5.80E-04**	**0**		∞	**<1E-6**
hsa-miR-205	252	4.17E-03	0		∞	<1E-6
hsa-miR-203	28	4.64E-04	0		∞	0.000009
hsa-miR-200c	**252**	**4.17E-03**	**2**	**6.09E-05**	**68.50**	**<1E-6**
hsa-let-7b	8094	1.34E-01	1419	4.32E-02	3.10	<1E-6
hsa-miR-17–5p	68	1.13E-03	13	3.96E-04	2.84	0.000168
hsa-miR-30d	8	1.32E-04	2	6.09E-05	2.17	0.510203
hsa-let-7a	11327	1.88E-01	3199	9.74E-02	1.92	<1E-6
hsa-miR-331	14	2.32E-04	4	1.22E-04	1.90	0.326997
hsa-miR-19b	154	2.55E-03	48	1.46E-03	1.74	0.000508
hsa-miR-224	35	5.80E-04	11	3.35E-04	1.73	0.123317
hsa-miR-106b	116	1.92E-03	38	1.16E-03	1.66	0.006686
hsa-miR-20a	182	3.01E-03	62	1.89E-03	1.60	0.001232
hsa-miR-19a	29	4.80E-04	10	3.05E-04	1.58	0.242926
hsa-let-7 g	78	1.29E-03	27	8.22E-04	1.57	0.041223
hsa-miR-18a	14	2.32E-04	5	1.52E-04	1.52	0.480909
hsa-miR-26a	13	2.15E-04	5	1.52E-04	1.41	0.626109
hsa-miR-29b	252	4.17E-03	100	3.05E-03	1.37	0.007234
hsa-miR-149	7	1.16E-04	3	9.14E-05	1.27	1
hsa-miR-101	7	1.16E-04	3	9.14E-05	1.27	1
hsa-miR-23a	106	1.76E-03	50	1.52E-03	1.15	0.450505
hsa-miR-424	54	8.94E-04	28	8.53E-04	1.05	0.908165
hsa-miR-25	28	4.64E-04	15	4.57E-04	1.01	1
hsa-miR-130a	88	1.46E-03	52	1.58E-03	0.92	0.65821
hsa-let-7f	3096	5.13E-02	1867	5.69E-02	0.90	0.000295
hsa-miR-29a	62	1.03E-03	38	1.16E-03	0.89	0.600658
hsa-let-7e	52	8.61E-04	32	9.75E-04	0.88	0.569916
hsa-miR-26b	26	4.31E-04	16	4.87E-04	0.88	0.747137
hsa-miR-100	29	4.80E-04	18	5.48E-04	0.88	0.649647
hsa-miR-382	8	1.32E-04	5	1.52E-04	0.87	0.778951
hsa-miR-495	7	1.16E-04	5	1.52E-04	0.76	0.763773
hsa-miR-369–3p	8	1.32E-04	6	1.83E-04	0.72	0.581543
hsa-miR-365	33	5.46E-04	25	7.62E-04	0.72	0.217416
hsa-miR-339	9	1.49E-04	7	2.13E-04	0.70	0.601483
hsa-miR-16	159	2.63E-03	124	3.78E-03	0.70	0.00275
hsa-miR-27a	239	3.96E-03	190	5.79E-03	0.68	0.000113
hsa-miR-222	163	2.70E-03	137	4.17E-03	0.65	0.00021
hsa-miR-103	143	2.37E-03	121	3.69E-03	0.64	0.000375
hsa-miR-34a	72	1.19E-03	62	1.89E-03	0.63	0.008563
hsa-miR-22	15	2.48E-04	13	3.96E-04	0.63	0.236842
hsa-miR-98	123	2.04E-03	108	3.29E-03	0.62	0.000319
hsa-miR-107	9	1.49E-04	8	2.44E-04	0.61	0.31794
hsa-miR-30b	46	7.62E-04	43	1.31E-03	0.58	0.014059
hsa-miR-21	1432	2.37E-02	1394	4.25E-02	0.56	<1E-6
hsa-let-7i	49	8.11E-04	49	1.49E-03	0.54	0.002895
hsa-miR-30a-5p	6	9.94E-05	6	1.83E-04	0.54	0.365183
hsa-miR-136	13	2.15E-04	14	4.26E-04	0.50	0.104627
hsa-miR-221	584	9.67E-03	629	1.92E-02	0.50	<1E-6
hsa-miR-143	8	1.32E-04	9	2.74E-04	0.48	0.134238
hsa-miR-191	22	3.64E-04	25	7.62E-04	0.48	0.013708
hsa-miR-125a	6	9.94E-05	7	2.13E-04	0.47	0.243234
hsa-miR-210	33	5.46E-04	39	1.19E-03	0.46	0.001179
hsa-let-7d	21	3.48E-04	25	7.62E-04	0.46	0.008358
hsa-miR-130b	10	1.66E-04	12	3.66E-04	0.45	0.072956
hsa-miR-15a	9	1.49E-04	11	3.35E-04	0.44	0.098035
hsa-miR-154	9	1.49E-04	11	3.35E-04	0.44	0.098035
hsa-miR-99b	46	7.62E-04	62	1.89E-03	0.40	0.000003
hsa-miR-409–3p	10	1.66E-04	14	4.26E-04	0.39	0.029933
hsa-miR-148b	10	1.66E-04	14	4.26E-04	0.39	0.029933
hsa-miR-15b	176	2.91E-03	251	7.65E-03	0.38	<1E-6

miRNA	No. of reads in PEC	Fraction of reads in PEC	No. of reads in PSC	Fraction of reads in PSC	Ratio: fraction of reads in PEC/fraction of Reads in PSC	Fisher's Exact Test *P*
hsa-miR-196b	4	6.62E-05	6	1.83E-04	0.36	0.110526
hsa-miR-324–5p	23	3.81E-04	36	1.10E-03	0.35	0.000058
hsa-let-7c	231	3.83E-03	371	1.13E-02	0.34	<1E-6
hsa-miR-24	174	2.88E-03	297	9.05E-03	0.32	<1E-6
hsa-miR-342	4	6.62E-05	8	2.44E-04	0.27	0.031964
hsa-miR-30c	4	6.62E-05	8	2.44E-04	0.27	0.031964
hsa-miR-125b	616	1.02E-02	1261	3.84E-02	0.27	<1E-6
hsa-miR-361	4	6.62E-05	11	3.35E-04	0.20	0.004478
hsa-miR-484	5	8.28E-05	17	5.18E-04	0.16	0.000069
hsa-miR-27b	54	8.94E-04	190	5.79E-03	0.15	<1E-6
hsa-miR-299–5p	2	3.31E-05	9	2.74E-04	0.12	0.002142
hsa-miR-199a*	3	4.97E-05	14	4.26E-04	0.12	0.000093
hsa-miR-152	5	8.28E-05	25	7.62E-04	0.11	<1E-6
hsa-miR-132	2	3.31E-05	16	4.87E-04	0.07	0.000004
hsa-miR-23b	2	3.31E-05	17	5.18E-04	0.06	0.000001
hsa-miR-199a	4	6.62E-05	260	7.92E-03	0.01	<1E-6
hsa-miR-199b	0	0.00E + 00	22	6.70E-04	0.00	<1E-6

To be included here, miRNAs were required to be represented by a total of at least 10 reads when reads in both datasets were summed. *MiR-141* and related family members are highlighted in bold. miRNAs are ranked in decreasing order of expression ratio, PEC/PSC.

Table 5. Description of commercially purchased RNA oligonucleotides used in standard curve and spike-in experiments

miRNA	Manufacturer of synthetic miRNA	Synthetic miRNA (oligo) sequence
miR-15b	Qiagen	AGCAGCACAUCAUGGUUUACA
miR-16	Qiagen	UAGCAGCACGUAAAUAUUGGCG
miR-19b	Qiagen	UGUGCAAAUCCAUGCAAAACUGA
miR-24	Qiagen	UGGCUCAGUUCAGCAGGAACAG
miR-141	Sigma	UAACACUGUCUGGUAAAGAUGG
miR-629[£]	IDT	GUUCUCCCAACGUAAGCCCAGC
miR-660	Sigma	UACCCAUUGCAUAUCGGAGUUG
cel-miR-39	Qiagen	UCACCGGGUGUAAAUCAGCUUG
cel-miR-54	Qiagen	UACCCGUAAUCUUCAUAAUCCGAG
cel-miR-238	Qiagen	UUUGUACUCCGAUGCCAUUCAGA

Note: The *miR-629** oligonucleotide corresponds to the sequence of *miR-629** in miRBase Release 10.1, but in some earlier releases of miRBase was formerly known as *miR-629*. Likewise, the Applied Biosystem *Taq*Man assays used to measure the *miR-629** sequence listed are in fact labeled as assays for *miR-629*. In our study, the sequence assayed for and used for generating standard curves is the one listed.

Table 6. Self-reported information for human donor blood samples used to generate results in Figs. 1 and 2 and Fig. S1 and Fig. S3

Sample ID	Gender	History of cancer
003	Female	No
006	Male	No
008	Male	No
013	Male	No
019	Male	No
021	Male	No

Table 7. Masses of frozen tumors collected from 12 mice from the first 22Rv1 xenograft cohort (i.e., the cohort used to generate data in Fig. 3)

Xenograft no.	Tumor mass, mg
1	959.5
2	206
3	917.6
4	778.9
5	801.3
6	1314.9
7	986.7
8	1119.8
9	641.6
10	411
11	2175.1
12	1208.6

These tumor mass data were used to generate results presented in Fig. S4.

Table 8. miRNA Taqman assays used in this study

miRNA	ABI item no.	miRNA *Taq*man assay target sequence
miR-15b	4373122	UAGCAGCACAUCAUGGUUUACA
miR-16	4373121	UAGCAGCACGUAAAUAUUGGCG
miR-19b	4373098	UGUGCAAAUCCAUGCAAAACUGA
miR-24	4373072	UGGCUCAGUUCAGCAGGAACAG
miR-100	4373160	AACCCGUAGAUCCGAACUUGUG
miR-125b	4373148	UCCCUGAGACCCUAACUUGUGA
miR-141	4373137	UAACACUGUCUGGUAAAGAUGG
miR-143	4373134	UGAGAUGAAGCACUGUAGCUCA
miR-205	4373093	UCCUUCAUUCCACCGGAGUCUG
miR-296	4373066	AGGGCCCCCCCUCAAUCCUGU
miR-629[c]	4380969	GUUCUCCCAACGUAAGCCCAGC
miR-660	4380925	UACCCAUUGCAUAUCGGAGUUG
cel-miR-39	4373455	UCACCGGGUGUAAAUCAGCUUG
cel-miR-54	4381162	UACCCGUAAUCUUCAUAAUCCGAG
cel-miR-238	4373437	UUUGUACUCCGAUGCCAUUCAGA

miRNA assays were designed against human miRNA sequences except for *cel-miR-39*, *cel-miR-54*, and *cel-miR-238*, which were designed against *C. elegans* miRNA sequences. Note that miRNA names and assay numbers provided are from the TaqMan qRT-PCR literature (Applied BioSystems), which uses miRNA nomenclature that predates the current miRBase release (v.10.1). In particular, *miR-629** as referenced throughout this article is listed as *miR-629* in some earlier miRBase releases and is likewise labeled as the TaqMan assay for *miR-629* in the Applied BioSystems literature.

Table 9. Results of TaqMan Low-Density array qRT-PCR profiling of human plasma from a healthy donor

miRNA	Ct value
hsa-miR-223–4373075	21.387175
hsa-miR-16–4373121	23.676111
hsa-miR-126–4378064	25.18676
hsa-miR-26a-4373070	25.349148
hsa-miR-24–4373072	25.352934
hsa-miR-19b-4373098	25.541594
hsa-miR-142–3p-4373136	25.777431
hsa-miR-92–4373013	26.029703
hsa-miR-26b-4373069	26.197817
hsa-miR-191–4373109	26.402868
hsa-miR-20a-4373286	26.709143
hsa-miR-146a-4373132	26.751621
hsa-miR-484–4381032	26.773163
hsa-miR-222–4373076	27.214977
hsa-miR-93–4373012	27.30701
hsa-miR-486–4378096	27.477003
hsa-miR-186–4373112	27.807243
hsa-miR-126–4373269	27.860714
hsa-miR-30b-4373290	28.025436
hsa-miR-15b-4373122	28.029036
hsa-miR-30c-4373060	28.051128
hsa-miR-19a-4373099	28.140797
hsa-miR-221–4373077	28.160389
hsa-miR-151–4373179	28.363777
hsa-miR-142–5p-4373135	28.433594
hsa-miR-103–4373158	28.643219
hsa-miR-17–5p-4373119	28.771618
hsa-miR-30a-5p-4373061	28.948341
hsa-miR-140–4373138	29.038239
hsa-miR-342–4373040	29.161871
hsa-miR-425–5p-4380926	29.179981
hsa-miR-27a-4373287	29.258652
hsa-miR-320–4373055	29.308796
hsa-miR-106b-4373155	29.49641
hsa-miR-374–4373028	29.52162
hsa-miR-30d-4373059	29.610056
hsa-miR-146b-4373178	29.699888
hsa-miR-432–4373280	29.779055
hsa-miR-197–4373102	29.831097
hsa-miR-331–4373046	29.86672
hsa-miR-127–4373147	29.948317
hsa-let-7 g-4373163	29.965107
hsa-miR-125a-4373149	29.986898
hsa-miR-328–4373049	30.116018
hsa-miR-301–4373064	30.40973
hsa-miR-382–4373019	30.51329
hsa-miR-21–4373090	30.570774
hsa-miR-28–4373067	30.670748
hsa-miR-425–4373202	30.68779
hsa-miR-20b-4373263	30.689703
hsa-let-7b-4373168	30.78085
hsa-miR-195–4373105	30.927505
hsa-miR-134–4373141	30.999826
hsa-miR-130a-4373145	31.000528
hsa-miR-130b-4373144	31.078936
RNU48–4373383	31.113333
hsa-miR-25–4373071	31.12904
hsa-miR-485–3p-4378095	31.133604
RNU48–4373383	31.251173
RNU48–4373383	31.336447
hsa-miR-411–4381013	31.392809
RNU48–4373383	31.430758
hsa-miR-335–4373045	31.442823
RNU48–4373383	31.452744
RNU48–4373383	31.479742
RNU48–4373383	31.515448
hsa-let-7a-4373169	31.531221
hsa-miR-181d-4373180	31.545853
hsa-miR-32–4373056	31.569336
hsa-miR-376a-4373026	31.573658
hsa-miR-152–4373126	31.622772
hsa-miR-532–4380928	31.661785
hsa-miR-451–4373209	31.692917
hsa-miR-324–3p-4373053	31.720333
hsa-miR-410–4378093	31.905563
hsa-miR-340–4373041	31.926765
hsa-miR-148a-4373130	31.928728
hsa-miR-199a-4378068	32.002617
hsa-miR-487b-4378102	32.159157
RNU48–4373383	32.170868
hsa-miR-224–4373187	32.18172
hsa-miR-18a-4373118	32.210087
hsa-miR-29a-4373065	32.36902
hsa-miR-30e-3p-4373057	32.405838
hsa-miR-200c-4373096	32.412086
hsa-miR-22–4373079	32.444557
hsa-miR-339–4373042	32.55535
hsa-miR-155–4373124	32.556374
hsa-miR-433–4373205	32.639957
hsa-miR-192–4373108	32.696526
hsa-miR-27b-4373068	32.729248
hsa-miR-99b-4373007	32.960518
hsa-miR-23b-4373073	32.97151
hsa-miR-491–4373216	33.038338
RNU44–4373384	33.05032
hsa-miR-423–4373015	33.054043
hsa-miR-133b-4373172	33.080162
hsa-miR-148b-4373129	33.082035
hsa-miR-383–4373018	33.127384
hsa-miR-15a-4373123	33.143764
hsa-miR-98–4373009	33.154266
hsa-miR-345–4373039	33.263832
hsa-miR-375–4373027	33.360348
hsa-miR-660–4380925	33.55976
hsa-let-7f-4373164	33.60402
hsa-miR-550–4380954	33.62478
RNU44–4373384	33.718765
RNU44–4373384	33.909008
hsa-miR-1–4373161	33.91329
hsa-miR-210–4373089	33.956635
hsa-miR-189–4378067	33.97108
RNU44–4373384	33.97398
hsa-miR-23a-4373074	34.062016
hsa-let-7d-4373166	34.074215
hsa-miR-424–4373201	34.11119
RNU44–4373384	34.251835
hsa-miR-493–4373218	34.25925
hsa-miR-29c-4373289	34.266956
hsa-miR-362–4378092	34.38831
hsa-miR-378–4373024	34.471447
hsa-miR-361–4373035	34.52986
hsa-miR-330–4373047	34.549976
hsa-miR-145–4373133	34.583946
RNU44–4373384	34.836792
hsa-miR-107–4373154	34.892826
hsa-miR-379–4373023	35.036655
hsa-miR-199a-4373272	35.053696
hsa-miR-196b-4373103	35.070187
hsa-miR-101–4373159	35.332664
hsa-miR-494–4373219	35.349953
hsa-miR-485–5p-4373212	35.529865
hsa-miR-183–4373114	35.559986

miRNA	Ct value
hsa-miR-326–4373050	35.68104
hsa-miR-572–4381017	35.794235
hsa-miR-657–4380922	35.9125
hsa-miR-30e-5p-4373058	35.951595
RNU44–4373384	36.030655
hsa-miR-7–4373014	36.180187
hsa-let-7c-4373167	36.44413
hsa-miR-17–3p-4373120	36.803318
hsa-miR-99a-4373008	37.132515
hsa-miR-181b-4373116	37.506042
hsa-miR-190–4373110	38.05101
hsa-miR-199b-4373100	39.025414
hsa-miR-181c-4373115	39.53926
hsa-let-7e-4373165	Undetermined
hsa-miR-10a-4373153	Undetermined
hsa-miR-10b-4373152	Undetermined
hsa-miR-34a-4373278	Undetermined
hsa-miR-34b-4373037	Undetermined
hsa-miR-34c-4373036	Undetermined
hsa-miR-141–4373137	Undetermined
hsa-miR-215–4373084	Undetermined
hsa-miR-218–4373081	Undetermined
hsa-miR-372–4373029	Undetermined
hsa-miR-9–4373285	Undetermined
hsa-miR-137–4373174	Undetermined
hsa-miR-200a-4373273	Undetermined
hsa-miR-125b-4373148	Undetermined
hsa-miR-296–4373066	Undetermined
hsa-miR-302a-4373275	Undetermined
hsa-miR-302c-4373277	Undetermined
hsa-miR-302d-4373063	Undetermined
hsa-miR-324–5p-4373052	Undetermined
hsa-miR-367–4373034	Undetermined
hsa-miR-369–5p-4373195	Undetermined
hsa-miR-449–4373207	Undetermined
hsa-miR-497–4373222	Undetermined
hsa-miR-501–4373226	Undetermined
hsa-miR-509–4373234	Undetermined
hsa-miR-510–4373235	Undetermined
hsa-miR-511–4373236	Undetermined
hsa-miR-514–4373240	Undetermined
hsa-miR-515–3p-4373241	Undetermined
hsa-miR-515–5p-4373242	Undetermined
hsa-miR-517a-4373243	Undetermined
hsa-miR-517b-4373244	Undetermined
hsa-miR-517c-4373264	Undetermined
hsa-miR-518a-4373186	Undetermined
hsa-miR-518b-4373246	Undetermined
hsa-miR-518c-4373247	Undetermined
hsa-miR-518d-4373248	Undetermined
hsa-miR-518e-4373265	Undetermined
hsa-miR-520a-4373268	Undetermined
hsa-miR-520b-4373252	Undetermined
hsa-miR-520c-4373253	Undetermined
hsa-miR-520d-4373254	Undetermined
hsa-miR-520e-4373255	Undetermined
hsa-miR-520f-4373256	Undetermined
hsa-miR-520 g-4373257	Undetermined
hsa-miR-520 h-4373258	Undetermined
hsa-miR-30a-3p-4373062	Undetermined
hsa-miR-95–4373011	Undetermined
hsa-miR-100–4373160	Undetermined
hsa-miR-132–4373143	Undetermined
hsa-miR-133a-4373142	Undetermined
hsa-miR-135a-4373140	Undetermined
hsa-miR-135b-4373139	Undetermined
hsa-miR-184–4373113	Undetermined

miRNA	Ct value
hsa-miR-194–4373106	Undetermined
hsa-miR-203–4373095	Undetermined
hsa-miR-204–4373094	Undetermined
hsa-miR-206–4373092	Undetermined
hsa-miR-211–4373088	Undetermined
hsa-miR-216–4373083	Undetermined
hsa-miR-217–4373082	Undetermined
hsa-miR-371–4373030	Undetermined
hsa-miR-381–4373020	Undetermined
hsa-miR-198–4373101	Undetermined
hsa-miR-299–5p-4373188	Undetermined
hsa-miR-31–4373190	Undetermined
hsa-miR-409–5p-4373197	Undetermined
hsa-miR-489–4373214	Undetermined
hsa-miR-506–4373231	Undetermined
hsa-miR-508–4373233	Undetermined
hsa-miR-521–4373259	Undetermined
hsa-miR-147–4373131	Undetermined
hsa-miR-149–4373128	Undetermined
hsa-miR-153–4373125	Undetermined
hsa-miR-187–4373111	Undetermined
hsa-miR-193a-4373107	Undetermined
hsa-miR-196a-4373104	Undetermined
hsa-miR-205–4373093	Undetermined
hsa-miR-208–4373091	Undetermined
hsa-miR-213–4373086	Undetermined
hsa-miR-214–4373085	Undetermined
hsa-miR-220–4373078	Undetermined
hsa-miR-325–4373051	Undetermined
hsa-miR-337–4373044	Undetermined
hsa-miR-380–3p-4373022	Undetermined
hsa-miR-422b-4373016	Undetermined
hsa-miR-182–4373271	Undetermined
hsa-miR-422a-4373200	Undetermined
hsa-miR-193b-4373185	Undetermined
hsa-miR-365–4373194	Undetermined
hsa-miR-429–4373203	Undetermined
hsa-miR-496–4373221	Undetermined
hsa-miR-500–4373225	Undetermined
hsa-miR-502–4373227	Undetermined
RNU6B-4373381	Undetermined
hsa-miR-105–4373157	Undetermined
hsa-miR-122a-4373151	Undetermined
hsa-miR-124a-4373150	Undetermined
hsa-miR-128b-4373170	Undetermined
hsa-miR-129–4373171	Undetermined
hsa-miR-139–4373176	Undetermined
hsa-miR-143–4373134	Undetermined
hsa-miR-182–4378066	Undetermined
hsa-miR-185–4373181	Undetermined
hsa-miR-18b-4373184	Undetermined
hsa-miR-200a-4378069	Undetermined
hsa-miR-202–4378075	Undetermined
hsa-miR-202–4373274	Undetermined
hsa-miR-299–3p-4373189	Undetermined
hsa-miR-302a-4378070	Undetermined
hsa-miR-302b-4378071	Undetermined
hsa-miR-302b-4373276	Undetermined
hsa-miR-302c-4378072	Undetermined
hsa-miR-329–4373191	Undetermined
hsa-miR-33–4373048	Undetermined
hsa-miR-369–3p-4373032	Undetermined
hsa-miR-376b-4373196	Undetermined
hsa-miR-380–5p-4373021	Undetermined
hsa-miR-412–4373199	Undetermined
hsa-miR-432–4378076	Undetermined
hsa-miR-512–5p-4373238	Undetermined

miRNA	Ct value
hsa-miR-9–4378074	Undetermined
hsa-miR-219–4373080	Undetermined
hsa-miR-323–4373054	Undetermined
hsa-miR-338–4373043	Undetermined
RNU44–4373384	Undetermined
hsa-miR-368–4373033	Undetermined
hsa-miR-373–4378073	Undetermined
hsa-miR-373–4373279	Undetermined
hsa-miR-448–4373206	Undetermined
hsa-miR-450–4373208	Undetermined
hsa-miR-452–4373281	Undetermined
hsa-miR-452–4378077	Undetermined
hsa-miR-453–4373210	Undetermined
hsa-miR-488–4373213	Undetermined
hsa-miR-490–4373215	Undetermined
hsa-miR-492–4373217	Undetermined
hsa-miR-503–4373228	Undetermined
hsa-miR-504–4373229	Undetermined
hsa-miR-505–4373230	Undetermined
hsa-miR-507–4373232	Undetermined
hsa-miR-513–4373239	Undetermined
hsa-miR-516–5p-4378099	Undetermined
hsa-miR-517–4378078	Undetermined
4343438-Blank	Undetermined
hsa-miR-518c-4378082	Undetermined
hsa-miR-518f-4378083	Undetermined
hsa-miR-519b-4373250	Undetermined
hsa-miR-519c-4373251	Undetermined
hsa-miR-519d-4373266	Undetermined
hsa-miR-519e-4373267	Undetermined
hsa-miR-522–4373245	Undetermined
hsa-miR-523–4373260	Undetermined
hsa-miR-524–4378087	Undetermined
hsa-miR-526b-4378080	Undetermined
hsa-miR-96–4373010	Undetermined
hsa-miR-651–4381007	Undetermined
hsa-miR-376a-4378104	Undetermined
hsa-miR-542–5p-4378105	Undetermined
hsa-miR-545–4380918	Undetermined
hsa-miR-544–4380919	Undetermined
hsa-miR-656–4380920	Undetermined
hsa-miR-549–4380921	Undetermined
hsa-miR-658–4380923	Undetermined
hsa-miR-652–4380927	Undetermined
hsa-miR-551a-4380929	Undetermined
hsa-miR-552–4380930	Undetermined
hsa-miR-553–4380931	Undetermined
hsa-miR-554–4380932	Undetermined
hsa-miR-555–4380933	Undetermined
hsa-miR-562–4380939	Undetermined
hsa-miR-563–4380940	Undetermined
hsa-miR-564–4380941	Undetermined
hsa-miR-565–4380942	Undetermined
hsa-miR-566–4380943	Undetermined
hsa-miR-551b-4380945	Undetermined
hsa-miR-569–4380946	Undetermined
hsa-miR-570–4380947	Undetermined
hsa-miR-548a-4380948	Undetermined
hsa-miR-586–4380949	Undetermined
hsa-miR-587–4380950	Undetermined
hsa-miR-548b-4380951	Undetermined
hsa-miR-588–4380952	Undetermined
hsa-miR-589–4380953	Undetermined
hsa-miR-591–4380955	Undetermined
hsa-miR-593–4380957	Undetermined
hsa-miR-594–4380958	Undetermined
hsa-miR-596–4380959	Undetermined
hsa-miR-597–4380960	Undetermined
hsa-miR-622–4380961	Undetermined
hsa-miR-599–4380962	Undetermined
hsa-miR-600–4380963	Undetermined
hsa-miR-624–4380964	Undetermined
hsa-miR-601–4380965	Undetermined
hsa-miR-626–4380966	Undetermined
hsa-miR-629–4380969	Undetermined
hsa-miR-548d-4381008	Undetermined
hsa-miR-639–4380987	Undetermined
hsa-miR-613–4380989	Undetermined
hsa-miR-614–4380990	Undetermined
hsa-miR-615–4380991	Undetermined
hsa-miR-616–4380992	Undetermined
hsa-miR-548c-4380993	Undetermined
hsa-miR-617–4380994	Undetermined
hsa-miR-642–4380995	Undetermined
hsa-miR-618–4380996	Undetermined
hsa-miR-644–4380999	Undetermined
hsa-miR-646–4381002	Undetermined
hsa-miR-647–4381003	Undetermined
hsa-miR-649–4381005	Undetermined
hsa-miR-650–4381006	Undetermined
hsa-miR-661–4381009	Undetermined
hsa-miR-662–4381010	Undetermined
hsa-miR-449b-4381011	Undetermined
hsa-miR-653–4381012	Undetermined
hsa-miR-654–4381014	Undetermined
4343438-Blank	Undetermined
hsa-miR-575–4381020	Undetermined
hsa-miR-576–4381021	Undetermined
hsa-miR-578–4381022	Undetermined
hsa-miR-579–4381023	Undetermined
hsa-miR-580–4381024	Undetermined
hsa-miR-585–4381027	Undetermined
hsa-miR-200b-4381028	Undetermined
hsa-miR-512–3p-4381034	Undetermined
hsa-miR-631–4380971	Undetermined
hsa-miR-363–4380917	Undetermined
hsa-miR-645–4381000	Undetermined
hsa-miR-659–4380924	Undetermined
hsa-miR-556–4380934	Undetermined
hsa-miR-558–4380936	Undetermined
hsa-miR-627–4380967	Undetermined
hsa-miR-630–4380970	Undetermined
hsa-miR-603–4380972	Undetermined
hsa-miR-606–4380974	Undetermined
hsa-miR-607–4380975	Undetermined
hsa-miR-608–4380976	Undetermined
hsa-miR-609–4380978	Undetermined
hsa-miR-633–4380979	Undetermined

Data were generated by using plasma from Individual 006; see Table S1 for additional information about the donor. Note that miRNA names and assay numbers provided are from the TaqMan TLDA qRT-PCR card literature, which uses miRNA nomenclature that predates the current miRBase release (v.10.1). The first column lists the miRNA name and Applied Biosystems TaqMan miRNA assay identifier. Values in the second column represented cycle threshold (Ct) values obtained from qRT-PCR analysis of the indicated miRNAs. miRNAs are listed in order of increasing Ct values.